REPORT DO(

AD-A238 861

Form Approved
OMB No. 0704-0188

Public reporting burden for this collection of information is estimated to average ... hour per response, including the time for reviewing instructions, searching existing data sources, gathering and maintaining the data needed, and completing and reviewing the collection of information. Send comments regarding this burden estimate or any other aspect of this collection of information, including suggestions for reducing this burden, to Washington Headquarters Services, Directorate for information Operations and Reports, 1215 Jefferson Davis Highway, Suite 1204, Arlington, VA 22202-4302, and to the Office of Management and Budget, Paperwork Reduction Project (0704-0188), Washington, DC 20503.

1. AGENCY USE ONLY (Leave blank)	2. REPORT DATE	3. REPORT TYPE AND DATES COVERED
	28 Jun 91	ANNUAL 01 Jun 90 to 31 May 91

4. TITLE AND SUBTITLE
Biological and Theoretical Studies of Adaptive Networks: The Conditioned Response

5. FUNDING NUMBERS
AFOSR-89-0391
PE - 61102F
PR - 2312
TA - A1

6. AUTHOR(S)
Dr John W. Moore

7. PERFORMING ORGANIZATION NAME(S) AND ADDRESS(ES)
Department of Psychology & Computer and Infor Science
Unviersity of Massachusetts
Amherst, MA 01003

8. PERFORMING ORGANIZATION REPORT NUMBER
AFOSR-TR 91 0644

9. SPONSORING/MONITORING AGENCY NAME(S) AND ADDRESS(ES)
Air Force Office of Scientific Research
Life Sciences Directorate
Building 410
Bolling AFB DC 20332-6448

NL

10. SPONSORING/MONITORING AGENCY REPORT NUMBER

11. SUPPLEMENTARY NOTES

12a. DISTRIBUTION/AVAILABILITY STATEMENT
Approved for public release;
distribution unlimited

12b. DISTRIBUTION CODE

13. ABSTRACT (Maximum 200 words)

The following experimental projects were initiated: (a) Reexamination of the activity of neurons of cerebellar cortex during two-tone differential conditioning (Dr. Iwona Zurawska). (b) A recording study of the medial geniculate neurons during two-tone differential trace conditioning (Dr. Kevin O'Connor). (c) A recording study of pontine nucleus neurons during two-tone differential conditioning (Michael Hirl). (d) Anatomical experiments using WGA-HRP designed to clarify red nucleus innervation of the cerebellum (Marcy Rosenfield). (e) A behavioral experiment designed to assess attenuated latent inhibition by "flagging", a phenomenon of potential importance for connectionist learning theories (Peter Underdown). In addition to the experimental work, my current team and I have initated a major upgrading of experimental facilities.

14. SUBJECT TERMS	15. NUMBER OF PAGES 59
	16. PRICE CODE

17. SECURITY CLASSIFICATION OF REPORT	18. SECURITY CLASSIFICATION OF THIS PAGE	19. SECURITY CLASSIFICATION OF ABSTRACT	20. LIMITATION OF ABSTRACT
(U)	(U)	(U)	UNLIMITED

NSN 7540-01-280-5500

Standard Form 298 (Rev. 2-89)
Prescribed by ANSI Std. Z39-18

June 30, 1991
Annual Technical Report No. 2
AFOSR 89-0391 (Adaptive Networks)
Dr. Geneviere Haddad, Ph. D., Program Manager

Biological and Theoretical Studies of Adaptive Networks: The Conditioned Response

Dr John W Moore (331-30-9491), Principal Investigator

Departments of Psychology and Computer and Information Science
Unversity of Massachusetts, Amherst 01003
Telephone 413-545-0569; FAX 413-545-0996

I. Summary

Investigations of adaptive neural networks were conducted using the classically conditioned nictitating membrane reponse (NMR) of rabbit, a widely used model system for studies of learning. Our work this past year involved neurobiological, behavioral, and theoretical approaches. The following experimental projects were initiated: (a) Reexamination of the activity of neurons of cerebellar cortex during two-tone differential conditioning (Dr. Iwona Zurawska). (b) A recording study of the medial geniculate neurons during two-tone differential *trace* conditioning (Dr. Kevin O'Connor). (c) A recording study of pontine nucleus neurons during two-tone differential conditioning (Michael Hirl). (d) Anatomical experiments using WGA-HRP designed to clarify red nucleus innervation of the cerebellum (Marcy Rosenfield). (e) A behavioral experiment designed to assess attenuated latent inhibition by "flagging", a phenomenon of potential importance for connectionist learning theories (Peter Underdown).

In addition to the experimental work, my current team and I have initated a major upgrading of experimental facilities. Basically, we now have three laboratories for single-unit recording in awake, behaving animals. Another laboratory contains two computer-controlled setups for doing behavioral experiments (i.e., no neuronal recording involved). All of these laboratories are based on technology of the 1970s. They are all based on 8-bit Apple II computers or their equivalent. These computers must be programmed in assembly language and consequently lack flexibilty and power for real-time control, data acquisition, and data manipulation. My current National Science Foundation grant (BNS 88-10624) has provided funds for developing new state-of-the-art laboratories based on the Intel 386 family of 32-bit microprocessors (e.g., as in Brainwave^{TM} workstations). One prototype system is presently being assembled and evaluated, and we hope to eventually replace all five laboratory computers.

This past year we submitted for publication several papers based on previous work. These papers were co-authored by me and members of my group who have moved on to other positions. All of these papers have either appeared during the past year or are "in press."

II. Research Objectives

The general objectives for the reporting period were the same as those stated in previous reports going back to those submitted in connection with AFOSR Grants 83-0215 and 86-0182. These goals and our approaches to them remain unchanged, so only a brief summary is presented here. Basically, we use the classically conditioned eye blink (nictitating membrane response—NMR) as a model system for theoretically oriented behavioral studies of learning. The theoretical orientation derives from connectionist algorithms used by our colleagues in computer science. These algorithms or models are real-time versions of the Widrow-Hoff "delta" learning rule. The specific models we have developed are closely related to models of Sutton and Barto.

III. Status of Research

The easiest way to describe the status of the research is to summarize the main research efforts of each individual working in my laboratory and under my general direction.

1. Dr. Iwona Zurawska, Ph. D.

Dr. Zurawska joined my group in mid-July 1990 after an eight-month postdoctoral stint at the University of Rochester. She returned to Poland in May in order to take a teaching position in the Department of Physiology of the Medical Academy of Bydgoszcz. While here, she conducted a study of neuronal activity of cerebellar cortex in rabbits trained in a two-tone differential conditioning task (which has been a standard protocol for several published reports from my laboratory dating from 1986). We were especially interested in lobulus simplex (HVI of Larsell) because this region of cerebellar cortex is essential for robust conditioned responding. She recorded from 160 cells, with 115 confirmed histologically in HVI. Of these, 59 showed activity related to conditioned responding. Surprizingly, 40 cells modulated their activity in relation to all three trial events: the conditioned stimuli, the conditioned response, and the unconditioned stimulus. Neurons with these characteristics are candidate loci for learning through Hebbian convergence of inputs. Eighteen of these cells are confirmed Purkinje cells because of the presence of both simple and complex spikes. Further histological and statistical analyses are planned in order to classify various cell types (Purkinje, granule, Golgi, basket).

2. Dr. Kevin O'Connor, Ph. D.

Dr. O'Connor's study of MGN neuronal activity during trace conditioning is only in it's preliminary stages. Unlike Dr. Zurawska, who was trained and experienced in electrophysiological recording from awake animals, his doctoral training was in animal behavior and cognitive psychology. During the past year he has learned surgical techniques, histology, microscopy, in addition to responsibilities which include maintenance of our local computer network and the design and assembly of laboratory components. Nevertheless, he has accummulated enough recording data to confirm published accounts (dating from the mid-1970s) of the the activity of MGN neurons during classical conditioning. This experimental literature indicates that a typical MGN cell responds to a reinforced conditioned stimulus (CS+) with a short-latency and short-duration increase in firing,

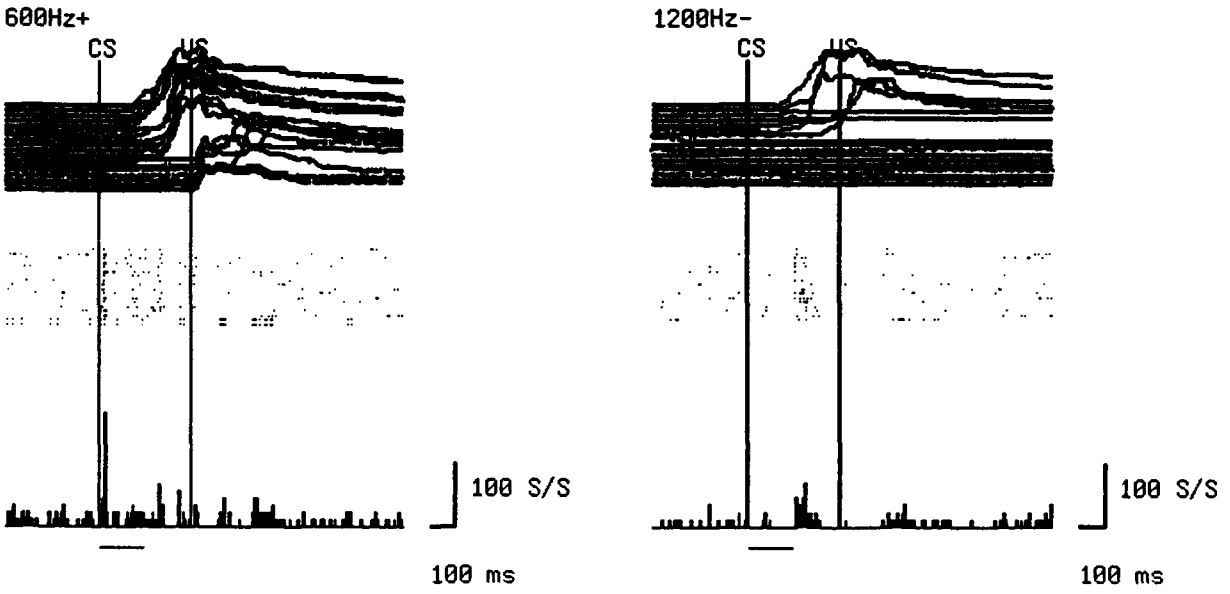

Figure 1. Raster plot and cell spike histogram on CS+ (600-Hz) and CS- (1200-Hz) trials. The vertical line marked "CS" indicates CS onset. The vertical line marked "US" indicates US onset. The top traces are the NMRs for each trial arranged in order of increasing onset latency. The middle sections are raster plots of the cell's spike activity arranged in the same order as the NMR traces. The bottom sections are histograms (spikes/sec) combined across trials for discrete intervals. CS duration is indicated by the horizontal lines under the histograms. Further details are in the text.

as illustrated in the accompanying figures. O'Connor is recording from neurons during trace conditioning. We are especially interested in whether MGN cells respond to the offset as well as the onset of the conditioned stimuli. This question is important for computational models of learning, particularly the tapped delay-line model of adaptive timing (VET model) described by Desmond and Moore in a series of articles in *Biological Cybernetics* and in chapters, e.g., "Implementing Connectionist Algorithms for Classical Conditioning in the Brain," which accompanies this report. Figure 1 summarizes data from an MGN neuron. This cell is interesting because it suggests that conditioned stimulus offset as well as onset triggers a burst of firing. This is consistent with the VET model.

3. Michael Hirl

Michael Hirl has just completed his first year of graduate studies in our Neuroscience and Behavior doctoral program. (He received grades of A in all of his course work: biochemistry, physiological psychology, psychopharmacology, neurobiology. In addition, he served as a teaching assistant.) His recording study of pontine nuclei is in its initial stages. Pontine nuclei contain neurons that project mossy fibers to cerebellar cortex. The activity of these cells during conditioned responding should tell us how information from conditioned stimuli is *represented* enroute to putative learning sites

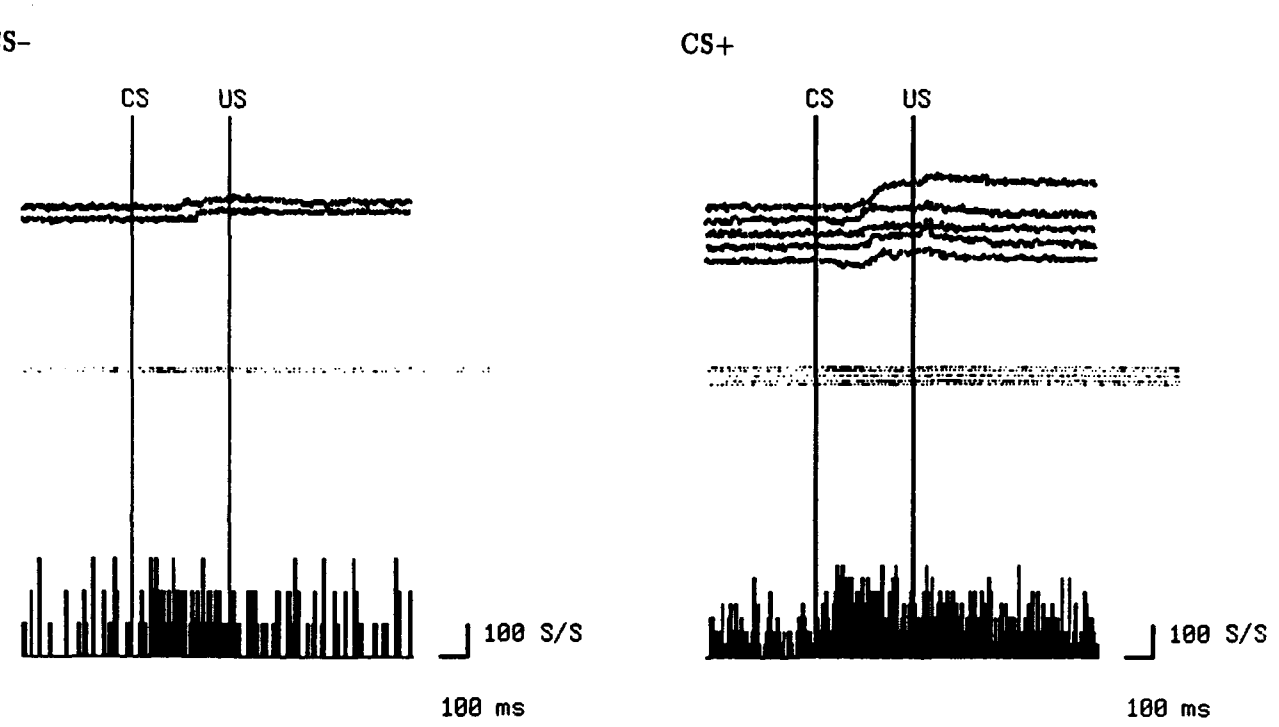

Figure 2. Raster plot and cell spike histogram for CS+ (1200-Hz) and CS- (600-Hz) trials. See Figure 1 caption and text for further details

in the cerebellum. As explained in the accompanying chapter, "Implementing Connectionist Algorithms...", one computational model and implementation scheme (Sutton-Barto-Desmond model) predicts that each pontine nuclear cell should firing in such a way as to provide the cerebellar cortex with a *template* of the conditioned response. Another computational model and implementation scheme, the tapped delay-line (VET) model assumes that each pontine nuclear cell fires with sustained burst of activity which begins with a constant latency with respect to the onset of the conditioned stimulus, but such that the latency of this burst varies by tens or hundreds of milliseconds from cell to cell. Representative data from a pontine nuclear cell are shown in Figure 2.

4. Marcy E. Rosenfield

Rosenfield is a research technician who has been associated with my laboratory for ten years. She has been investigating brain stem and cerebellar circuits involved in the conditioned NMR using implanted WGA-HRP has a marker. We shall be presenting a poster at this year's Society for Neuroscience meetings describing afferent connections from the red nucleus to the cerebellar cortex. Cerebellar cortex (Larsell's HVI) has been implicated in the generation of the classically conditioned eye blink/NMR. The motor program for the conditioned response is presumably learned by the cerebellum and relayed to motoneurons via the red nucleus (e.g., Rosenfield, M. & Moore, J., *Behav Brain Res*, 10:393, 1983). Projections from the red nucleus to HVI could be important for brain stem and cerebellar processes involved in classical conditioning (e.g., Moore, J. et al, *Biol Cyber*, 62:17, 1989). WGA-HRP was implanted unilaterally into HVI. We restricted consideration to those cases showing retrogradely labeled cells in the pontine nuclei, spinal trigeminal nucleus par oralis, and the dorsal accessory olivary nucleus, as these structures are known to project to HVI.

All such cases showed sparse retrogradely labeled cells in the more caudal (3rd nerve level) portions of the red nucleus, consistent with Dietrich and Walberg's cat study (Dietrichs, E. & Walberg, F., *Exp Brain Res*, 50:353, 1983).

5. Peter Underdown

Peter Underdown is a computer science graduate student who conducted experiments to determine whether "flagging" a potential conditioned stimulus (a tone, T) by preceding it repeatedly with a brief light (L) would enhance subsequent conditioning of the NMR to the tone. Before experiencing NMR conditioning, animals were given one of three treatments: (a) L repeatedly preceded T by a few hundred milliseconds (L-T); (b) L and T were repeatedly presented but unpaired (L/T); (c) L but not T was repeatedly presented (L-alone). All of these treatments were followed by training in which T was paired with the unconditioned stimulus. Previous experiments suggested that L-T treated animals acquire a conditioned NMR more quickly than L/T treated animals (the "flagging" effect). Is "flagging" a genuine facilitation effect or merely an attentuation of latent inhibition? (Latent inhibition is the technical term for retarded acquisition of a conditioned response following a series of preexposures to the conditioned stimulus.) The addition of the L-alone treatment as a control allowed us to answer this question. If "flagging" is the result of enhancement, then the L-T treatment ought to result in faster NMR conditioning than the L-alone treatment. If on the other hand the L-T treatment attenuates latent inhibiton, then the L-alone treatment ought to result in faster conditioning than the L-T treatment. After some preliminary pilot experiments, a full-scale study was conducted by Underdown using the basic three-group design (N = 12/group). He found that the L-alone treatment resulted in *faster* NMR conditioning than either the L/T or the L/T treatments. This result indicates that the "flagging" effect is due to attentuated latent inhibition and not enhancement.

IV. Technical Reports

Included are published and submitted work initiated under AFOSR Grant 86-0182 and partially supported by NSF. Items listed in prior reports are not included unless the previous citations were incomplete because they were "in press" or under review. For expediency, this list overlaps somewhat with one submitted with the final technical report for AFOSR 86-0182.

1. Rosenfield, M.E. and Moore, J.W. Red nucleus projections to the accessory abducens nucleus in rabbit reexamined with WGA-HRP. *Society for Neuroscience Abstracts*, 1990, 16, 271.

2. Berthier, N.E. and Moore, J.W. Orbicularis oculi and extraocular muscle activity during unconditioned and conditioned eyeblinks in the rabbit. *Society for Neuroscience Abstracts*, 1990, 16, 916.

3. Moore, J.W., Berthier, N.E., and Blazis, D.E.J. Classical eye blink conditioning: Brain systems and implementation of a computational model. In Gabriel, M. and Moore, J.W. (Eds.) ***Learning and Computational Neuroscience: Foundations of Adaptive Networks.*** Cambridge, MA: Bradford Books/MIT Press, 1990, pages 359-387.

4. Gabriel, M. and Moore, J.W. (Eds.) *Learning and Computational Neuroscience: Foundations of Adaptive Networks.* Cambridge, MA: Bradford Books/MIT Press, 1990. (613 pages)

5. Berthier, N.E. and Moore, J.W. Activity of deep cerebellar nuclear cells during classical conditioning of nictitating membrane extension in rabbits. *Experimental Brain Research*, 1990, 83: 44-54.

6. Moore, J.W. Implementing connectionist algorithms for classical conditioning in the brain. In Commons, M., Grossberg, S., and Staddon (Eds.) *Neural Network Models of Conditioning and Action.* Hillsdale, NJ: Lawrence Erlbaum Associates, 1991, pages 181-191.

7. Blazis, D.E.J. and Moore, J.W. Conditioned stimulus duration in classical trace conditioning: test of a real-time computational model. *Behavioural Brain Research*, 1991, 43, 73-78.

8. Desmond, J.E. and Moore, J.W. Activity of red nucleus neurons during the classically conditioned rabbit nictitating membrane response. *Neuroscience Research*, 1991, 10, 260-279.

9. Moore, J.W. and Desmond, J.E. A cerebellar neural network implementation of a temporally adaptive conditioned response. In Gormezano, I. (Ed.) *Learning and Memory: The Biological Substrates.* Hillsdale, NJ: Lawrence Erlbaum Associates. In press.

10. Desmond, J.E. and Moore, J.W. Altering the synchrony of stimulus trace processes: Tests of a neural-network model. *Biological Cybernetics.* In press.

11. Berthier, N.E., Barto, A.G., and Moore, J.W. Linear systems analysis of the relationship between firing of deep cerebellar neurons and the classically conditioned nicitating membrane response in rabbits. *Biological Cybernetics.* In press.

12. Richards, W.G., Ricciardi, T.N., and Moore, J.W. Activity of spinal trigeminal pars oralis and adjacent reticular formation neurons during the classically conditioned rabbit nictitating membrane response. *Behavioural Brain Research.* In press.

13. Rosenfield, M.E. and Moore, J.W. Red nucleus projections to cerebellar cortex (HVI) in rabbit examined with WGA-HRP. *Society of Neuroscience Abstracts*, 1991, 17. In press.

14. Blazis, D.E.J. and Moore, J.W. Conditioned inhibition of the nictitating membrane response in rabbits following hypothalamic and mesencephalic lesions. *Behavioural Brain Research.* Accepted pending revisions.

15. Moore, J. W. Memory structures in classical conditioning: Declarative and procedural knowledge in temporally adaptive behavior. To appear in L. Squire and N. Butters (Eds.) *Neuropsychology of Memory, 2nd Edition*, New York: Guilford.

V. Professional personnel

1. John W. Moore, Ph. D. (Psychology, Indiana) Principal Investigator.

2. Neil E. Berthier, Ph. D. (Psychology, UMass) Senior postdoctoral associate. Berthier had been associated with the lab for many years. He is presently associated with the department of computer and information science, a position he assumed in August, 1990.

3. John E. Desmond, Ph. D. (Psychology, UMass) Senior postdoctoral associate. Desmond had also been associated with the lab for many years. He is presently with EEG Systems Labs, Inc. of San Francisco, a position he assumed last January

4. Iwona Zurawska, Ph. D. (Natural Science, Nencki Institute, Warsaw, Poland) Postdoctoral associate. Zurawska joined the project in July, 1990 and returned to Poland May, 1991 to assume an academic position in physiololgy.

5. Kevin O'Connor, Ph. D. (Psychology, Columbia University) Postdoctoral fellow. O'Connor joined the laboratory in July, 1990.

6. Marcy E. Rosenfield, B.S. (Zoology, UMass) Departmental Assistant. Rosenfield is a certified AALAS animal care technician.

VI. Interactions (John W. Moore)

1. Participant at the Winter Conference on Animal Learning and Behavior, Winter Park, Colorado, January, 1991.

2. Presentations at meetings: Society for Neuroscience meetings in St. Louis, 1990.

4. Reviewing and Related Activity: Consulting editor for *Psychobiology* and reviewed manuscripts for several journals, including *Behavioural Brain Research*, Psychological Review, *Behavioral Neuroscience*.

5. Continuing interactive relationships with A G Barto and other colleagues working in Adaptive Networks: A H Klopf's group at AF Wright Avionics Lab, R S Sutton at GTE Labs, J C Houk and N A Schmajuk of Northwestern University, E J Kehoe of the University of New South Wales, and others.

VIA. Interactions (Kevin O'Connor)

Kevin O'Connor joined my laboratory one year ago after a post-doctoral stint at the University of Rochester. He is presently collaborating with P. Tallal and H. Fitch of the Rutgers University Center for Molecular and Behavioral Neuroscience on a project concerning the development of cerebral asymmetries in auditory processing in rats. In addition, he is coauthor of some recent and pending publications.

1. Ison, J. R., G. P. Bowen, and O'Connor, K. Reflex modification produced by visual stimuli in the rat following functional decortication. *Psychobiology*, 1991, 19, 122-126.

2. Ison, J. R., O'Connor, K., Bowen, G. P., and Bocirnea, A. Temporal resolution of gaps in noise by the rat is lost with functional decortication. *Behavioral Neuroscience*, 1991, 105, 33-40.

3. O'Connor, K. Ison, J. R. Echoic memory and tonal discrimination in the rat: Effects of inspection time, retention interval, and the spectral composition of retroactive noise. *Journal of Experimental Psychology: Animal Behavior Processes*, in press.

VII. New Discoveries

Discoveries that might be designated as new were those stemming from experimental research.

Exp Brain Res (1990) 83:44–54

Experimental Brain Research

Activity of deep cerebellar nuclear cells during classical conditioning of nictitating membrane extension in rabbits

N.E. Berthier and J.W. Moore

Department of Psychology, University of Massachusetts, Amherst, MA 01003, USA

Received December 19, 1989 / Accepted June 30, 1990

Summary. The activity of neurons in the interposed and dentate nuclei of the cerebellum was investigated during differential classical conditioning of the rabbit eye blink/nictitating membrane response. Forty-seven percent of the 165 cells in the study responded to the orbital stimulation used as the unconditioned stimulus (US). The latency distribution of US-elicited responses was bimodal with peaks at 7 and 19 ms. Twenty-one percent of the cells responded with short latencies to the tones used as conditioned stimuli (CSs). These cells typically responded to both the reinforced and nonreinforced CSs. Forty-one percent of the cells responded on conditioned response (CR) trials but not on trials without CRs. The average lead of the neural response to the CR was 71.4 ms. Cells that responded on CR trials were more likely to respond to the CSs, or to the CSs and the US, than cells that did not respond on CR trials. For about half of the cells that responded on CR trials the latency of response followed trial-by-trial variations of CR latency. For the remainder, the response was time-locked to CS-onset. Cells whose responses paralleled the CR may be involved in the initiation or modulation of the CR, while those whose responses were time-locked to the CS may be involved in sensory processing underlying the initiation of the movement. The pathways that may underlie the US- and CS-elicited responses are also discussed.

Key words: Nictitating membrane Cerebellar deep nuclear activity Learned movements Classical conditioning Eye blink Rabbit

Introduction

Research into the role of the cerebellum in motor learning has recently focused on vestibulo-ocular reflex gain modification (Ito, 1984; Lisberger, 1988; Miles et al., 1980), eye blink gain modification (Evinger and Manning, 1988), and classical conditioning of the nictitating membrane (NM) response (e.g., Moore and Berthier, 1987; Thompson, 1986; Yeo et al., 1985a). The NM response is one component of the eye blink, consisting of passive extension of the NM as the eyeball retracts. However, there is as yet no consensus on the role of the cerebellum in providing for these behavioral adaptations. The present paper reports on the activity of deep cerebellar nuclear cells during classical conditioning of the rabbit NM response. In this preparation eye blinks are conditioned using periorbital electrical stimulation or air puffs as unconditioned stimuli (USs), and NM position is measured as the conditioned response (CR). Auditory and visual stimuli are typically used as conditioned stimuli (CSs). McCormick et al. (1982c) showed that NM and eye blink amplitudes are highly correlated during conditioning.

The rabbit NM preparation has been widely used in the study of the physiological basis of classical conditioning. McCormick et al. (1982a) focused interest on the role of the cerebellum in NM conditioning by showing that lesions of interpositus and medial dentate disrupt CRs. The importance of an intact cerebellum was subsequently confirmed by studies showing that lesions of the cerebellum, its afferents, and its efferents have profound effects on conditioned eye blinks. Lesions of cerebellar cortex (Yeo et al. 1985b), red nucleus (Rosenfield and Moore 1983), superior cerebellar peduncle (McCormick et al. 1982b), and inferior olive (Türker and Miles 1986; Yeo et al. 1986) all disrupt conditioned responding.

Rather than impinging directly on circuits essential for generating CRs, lesions might disrupt NM conditioning indirectly because lesions of the cerebellum and its afferents can produce abnormal activity in efferent targets. For example, lesions of the inferior olive produce substantial reductions in neural firing in the cerebellar deep nuclei and the red nucleus (Billard et al. 1988; Strata 1985). Thus, it is possible that cerebellar lesions disrupt NM CRs by disrupting red nuclear activity that might be involved in conditioning (Tsukahara et al. 1981; Desmond and Moore

Offprint requests to: J.W. Moore (address see above)

1987). However, there are now ample data showing CR-correlated activity from single neurons in cerebellar cortex (Berthier and Moore 1986; Foy and Thompson 1986) and cerebellar deep nuclei (McCormick and Thompson 1984) to indicate that the cerebellum is probably involved in generating or modulating CRs.

Anatomical data implicate the anterior regions of the cerebellar posterior lobe in classical NM conditioning. Yeo et al. (1985a) concluded that lesions of hemispheral lobule VI abolish conditioning. On the other hand, Lavond et al. (1987) found that lesions of lobule VI disrupted retention but did not block reacquisition of the NM CR. Recording studies of the posterior lobe indicate a wealth of activity correlated with conditioning. Berthier and Moore (1986) studied Purkinje cell activity in intermediate and medial lateral zones of lobule VI and neighboring lobules during rabbit NM conditioning. We found many cells that showed changes in activity related to the performance of CRs. The changes in activity antedated initiation of movement by 20 to 100 ms in most cells. Some of the CR-related neurons also responded to the CSs and US used in conditioning.

The intermediate and medial lateral zones of lobule VI and surrounding lobules project to nucleus interpositus and medial dentate which project out of the cerebellum. The present investigation examined the activity of interpositus and medial dentate cells during classical conditioning. Of primary interest was whether the deep nuclear cells showed patterns of activity that are consistent with a causal role in generating CRs. Such activity should precede and be highly correlated with the CR. The response of cells to the stimuli used in conditioning was also of interest. If the cerebellum is a site of learning, then some cerebellar neurons, be they cortical or deep nuclear, should receive converging inputs conveying CS and US information. The present paper describes the response of nucleus interpositus and medial dentate cells to stimulation of the periorbital tissues, to the auditory stimuli used in conditioning and examines the modulation of neural activity cells during CRs.

Methods

Behavioral training

Twenty-six adult albino rabbits (3.5 to 4.5 kg) were trained in a differential classical conditioning paradigm. Tones of 1200 Hz and 600 Hz were used as CSs (75 dB re 20 $\mu N/m^2$ intensity). The reinforced (CS+) and nonreinforced tones (CS−) were presented in pseudorandom order. The intertrial interval was 20 s. This training protocol yields differential responding to the CS+ and CS−. The CS+ was always followed by the US, and the CS− was presented alone. CSs were counterbalanced across animals, i.e., the 1200-Hz tone was CS+ for one animal, and the 600-Hz tone was CS+ for the next animal. The CSs were 350 ms in duration. A single 0.1–1.0 mA DC pulse of 0.1–0.5 ms duration served as the US. Its intensity was adjusted to be as low as possible while still supporting conditioning. Two 9-mm stainless steel wound clips crimped into the skin surrounding the eye, one located in an inferior position within 3 mm of the margin and the other in a temporal position, also within 3 mm of the margin, served as electrodes for delivery of the US. The interval between the onset of CS+ and the US was 350 ms.

Movement of the right NM was measured by a minitorque potentiometer connected to the NM by a suture. Extensions of the NM during the CS-US interval were defined as CRs. Animals were required to meet a criterion of 90% CRs to the CS+ before surgery. Pretraining usually required 200 to 400 trials, i.e., 100 to 200 CS+ trials.

Surgery and recording

In preparation for surgery, an intravenous cannula was placed in the marginal ear vein, and an intravenous drip of lactated Ringer's solution was started. Anesthesia was induced by injection of sodium pentothal in the side port of the infusion set. The pentothal was given to effect and repeated at intervals of 5 to 10 min. Lidocaine was injected subcutaneously at the areas of contact between the head and the stereotaxic frame and along the skull midline. The animal was then placed in a stereotaxic frame and the midline skin was incised to expose the skull. Three stainless steel bolts were then implanted into the right frontal and right and left parietal bones. After the bolts were implanted an opening (approximately 4 mm × 8 mm) was made in the right occipital bone which exposed the dura mater overlaying the right cerebellar hemisphere. A dental cement cap was then built up on the skull with the occipital bone opening left exposed. An American National Standard 1/2–13 threaded stainless steel rod was embedded in the dental cement cap for fixing the head during recording (the rod was 12.5 mm in diameter with 13 threads per 2.54 cm and approximately 4 cm in length). The rod protruded from the cement cap by approximately 2 cm, and was implanted at an angle of 25° to the stereotaxic vertical so that the rabbit's head was pitched forward 25° during recording. The opening over the cerebellum was covered with sterile Gelfoam. The total amount of time the animal was generally anesthetized during this procedure was 1.5–3.0 min. The animal was then placed in a holding box and allowed to recover for at least two hours. It was then placed in the apparatus and tested for CRs. Most animals began making CRs within the first 20 trials (i.e., about 10 CS+ trials). If the animal did not make CRs within 100 trials they were removed from the apparatus and placed in the holding box for another hour. All animals made CRs after this subsequent recovery period. Data were obtained from an animal during two or three recording sessions. The recording sessions for a given animal occurred on a single day, with the animal being returned to a holding box between sessions. The opening over the cerebellum was rinsed with sterile saline between sessions and sealed with sterile Gelfoam.

During recording sessions rabbits were loosely restrained in a Plexiglas box with their head affixed to an aluminum frame by the implanted threaded rod. The Gelfoam overlaying the cerebellum was removed and the dura rinsed with saline. The dura was then incised to allow for glass microelectrodes to be introduced into the cerebellum. Single units were recorded with microelectrodes filled with 2 M NaCl and saturated with FCF green dye. Recording sites were marked by ionophoresis of the FCF green dye by passing a 12-μA current for 5 to 10 min (electrode negative). Nictitating membrane position data and cell activity were amplified and recorded on a Vetter Co. modified VCR (Model 420).

After the last recording session the animal received a lethal injection of sodium pentobarbital and was perfused through the aorta with isotonic saline followed by 10% formaldehyde solution. The brain was then removed from the skull and frozen sections were cut at 60 microns and mounted and stained with cresyl violet.

Data analysis

Recorded neural activity was window discriminated and fed to an Apple IIe computer. The computer detected discriminator pulses and noted the time of each pulse relative to the start of the trial (i.e., 350 ms prior to CS onset). At the same time, analog signals from the

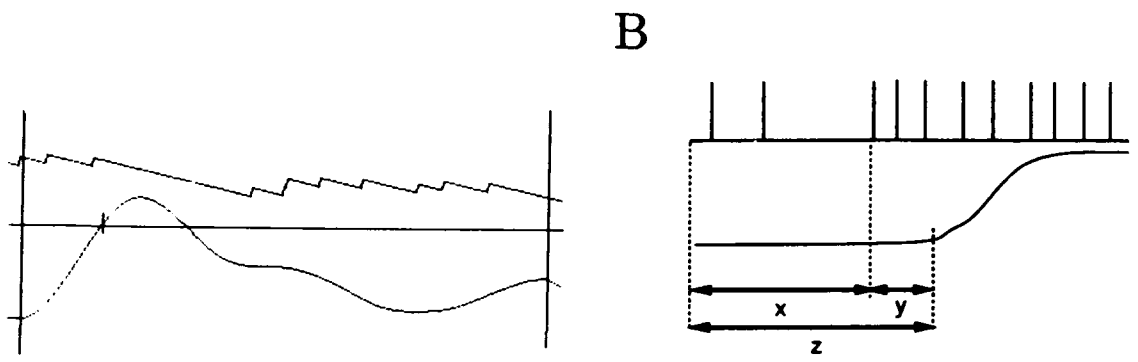

Fig. 1. A An example of the filtering procedure for determining change-points in neural firing (cell 52a). The top trace is the cumulative sum of spike activity and the bottom trace is filtered spike activity (Eq. 1). The two long vertical lines indicate CS and US onset. The time between CS and US onset is 350 ms. The short vertical line in the filtered data indicates the zero-crossing (firing change-point). In the cumulative sum trace, the small upward deflections correspond to individual action potentials. Since the cumulative sum was adjusted for the mean pre-CS firing rate of the neuron, prolonged periods of negative slope indicate a time in which firing of the cell decreased below the pre-CS level. **B** An illustration of the three variables used to compute VR. Variable x is the difference between the stimulus onset and spike-change times. Variable y is the difference between spike-change and CR onset. Variable z is the difference between CS and CR onset

NM transducer were digitized with an eight-bit A/D converter. Data were stored on floppy disks, eventually to be sent to a Sun Microsystems computer where they were stored on disk. Periresponse-time histograms, peristimulus-time histograms and rasters were generated for each unit. The histograms and rasters could be based on CS+ trials, CS− trials, trials on which CRs occurred, trials on which no CRs occurred, or all trials.

In order to assess whether a cell showed short latency responses to the CSs, its activity immediately before and after CS onset was compared. Pre- and post-CS interspike interval distributions were generated from recordings 100 ms before and after CS onset averaged over both CS+ and CS− trials. The interspike interval distributions were then compared with a two-tailed Kolmogorov-Smirnov test ($\alpha = 0.05$). Since the experiment-wise Type I error rate would be high using this procedure, peristimulus-time histograms of units with significant Kolmogorov-Smirnov outcomes were examined to ensure that the response was reliable and discernible.

A similar procedure to detect changes in firing before and during CRs was used. Conditioned response onset was easily determined because of the low variability in the NM baseline position. Conditioned response onset was defined as the earliest time following CS onset that NM position was one standard deviation (SD) plus 2 A/D units away from the pre-CS position mean. A distribution of interspike intervals was then generated for the period of 150 ms before and 50 ms after CR onset. This distribution was then compared with the distribution of interspike intervals before CS onset using a two-tailed Kolmogorov-Smirnov test ($\alpha = 0.01$). Histograms and rasters were then visually examined to confirm the statistical decision. Cells that met these criteria were called CR-related.

We determined the time of changes of neural firing rate using an edge-detection digital filter after Marr and Hildreth (1980). In the first step of this procedure, the cumulative sum of spike activity was low-pass filtered by convolving with a Gaussian. The cumulative sum for the jth time step was equal to $\Sigma_{i=0}^{j}(g_i - \bar{g})$, where g was an impulse sequence respresenting spike activity and $\bar{g}$ the mean number of spikes per time step in the pre-CS period. The time step was 1 ms.

The low-passed data were then differentiated to obtain firing frequency. These data were then passed through a third stage where the second derivative of the firing frequency was calculated. The points where firing frequency changed (the change-points) were then estimated by taking the zero-crossing of the output.

Specifically, the filter was designed as follows:

$$f(x) = D^2[D(G * g)](x),$$

where $*$ is the convolution operator, D the derivative operator, g the input to be filtered, f the filtered output. G is the Gaussian function $G(x) = [1/\sigma(2\pi)^{1/2}]\exp(-x^2/(2\sigma^2))$. This yields

$$f(x) = (D^3G * g)(x)$$

by the associative and derivative properties of convolutions. Completing the differentiation,

$$f(x) = [(-1/\sigma^3(2\pi)^{1/2})(-x/\sigma^2 - 2x/\sigma^2 + x^3/\sigma^4)\exp(-x^2/2\sigma^2)] * g(x). \quad (1)$$

In practice D^3G was sampled at 1-ms intervals and convolved with the cumulative sum of spike activity. σ was set at 2.4 for all cells. The slope of f at the zero-crossing is proportional to the degree of change in firing rate (Marr and Hildreth 1980). The cumulative sum of spike activity and f were displayed on a graphics terminal and an operator could set a criterion for the slope at the zero-crossing above which the change-point was accepted as significant. The slope criterion was set at the same value for all trials for a given cell. An example of this procedure is shown in Fig. 1A for the cell whose rasters are shown in Fig. 9. The top trace of Fig. 1A shows the cumulative sum of spike activity and the bottom trace shows the filtered activity. This cell showed a decrease in firing when the CS was presented. The change-point in firing was defined as the zero-crossing of the filtered activity and is indicated by the vertical line.

Once CR and spike-change onset times were obtained, the data was analyzed to determine if the unit was showing movement or stimulus related firing. Movement related activity was defined as activity whose onset time followed trial-by-trial variations in CR onset time. Stimulus related activity was defined as activity that did not shift when the CR shifted, but was time-locked to CS onset. *Movement or stimulus relatedness* was quantified using three variables: Variable x was the difference between the stimulus onset and spike-change times. Variable y was the difference between spike-change and CR onset. Variable z was the difference between CS and CR onset. These three variables are illustrated in Fig. 1B.

One would expect the Pearson correlation coefficient between x and z (r_{xz}) to be high if activity was movement related and r_{yz} to be high if the activity was stimulus related (Lamarre et al. 1983). However, Commenges and Seal (1986) point out that if the r_{xy} is also positive one cannot simply compare r_{xz} and r_{yz} to determine if the activity is stimulus or movement related. To determine stimulus or movement relatedness, they suggest the use of the variance ratio (VR), σ_y^2/σ_x^2. If the cell is movement related, VR should be less than 1.

If it is stimulus related, VR should be greater than 1. VRs were computed for all CR-related cells.

Results

Recording locations

Electrode placement was guided by the characteristic electrical activity of different cerebellar areas. Examination of dye marks made at recording locations showed only infrequent recording locations outside the deep nuclei. One hundred sixty-five cells were located in the deep nuclei and the immediately surrounding regions, five in the cerebellar white matter, and six in the brainstem. Only the cells from the deep nuclei and the immediately surrounding regions are discussed in this paper. Figure 2 shows recording locations of these cells. Two units were recorded in the lateral zone of the fastigial nucleus, 93 in nucleus interpositus anterior (NIA), 11 in nucleus interpositus posterior, 34 in medial dentate, nine ventrally bordering interpositus, and 16 ventrally bordering dentate.

While the possibility of recording from cerebellar cortical afferents and efferents cannot be ruled out, the data suggest that the vast majority of recordings were from cell bodies. No units could be recorded until electrodes were 1 to 2 mm below the lowest cortical layer. This suggests that electrodes did not generally record activity in areas where only axons were present.

Spontaneous unit activity

Unit spontaneous activity was computed from the 350-ms period preceding CS onset and averaged across trials. The mean firing frequency across cells was 60.1 impulses/s (SD = 26.9; coefficient of variability $\left[\frac{\textit{interspike interval SD}}{\textit{interspike interval mean}}\right]$ = 0.51). The mean firing frequency of about 60 impulses/s for deep nuclear units is slightly faster than those reported for the cat or monkey which range from 42 to 56 impulses/s (Armstrong and Edgley 1984; Chapman et al. 1986; Cody et al. 1981). This comparatively higher rate of firing may be because baseline rates were estimated during the 20-s intervals between trials or it may be a result of species differences. With short intertrial intervals there is the likelihood that preceding trials influence the firing rate during the pre-trial measurement period.

Neural responses to the US

Examination of peristimulus-time histograms and rasters indicated that 77 cells (47% of the total) responded to the US. Figure 3 shows the response of four cells to the US. The arrow indicates the onset of the stimulus pulse and the filled square below each trace indicates the first spike that was evoked by the US. The latency of the responses ranged from 10 to 13 ms in these four cells.

The activity of the 77 US-responsive cells was examined on an oscilloscope to determine the onset latency

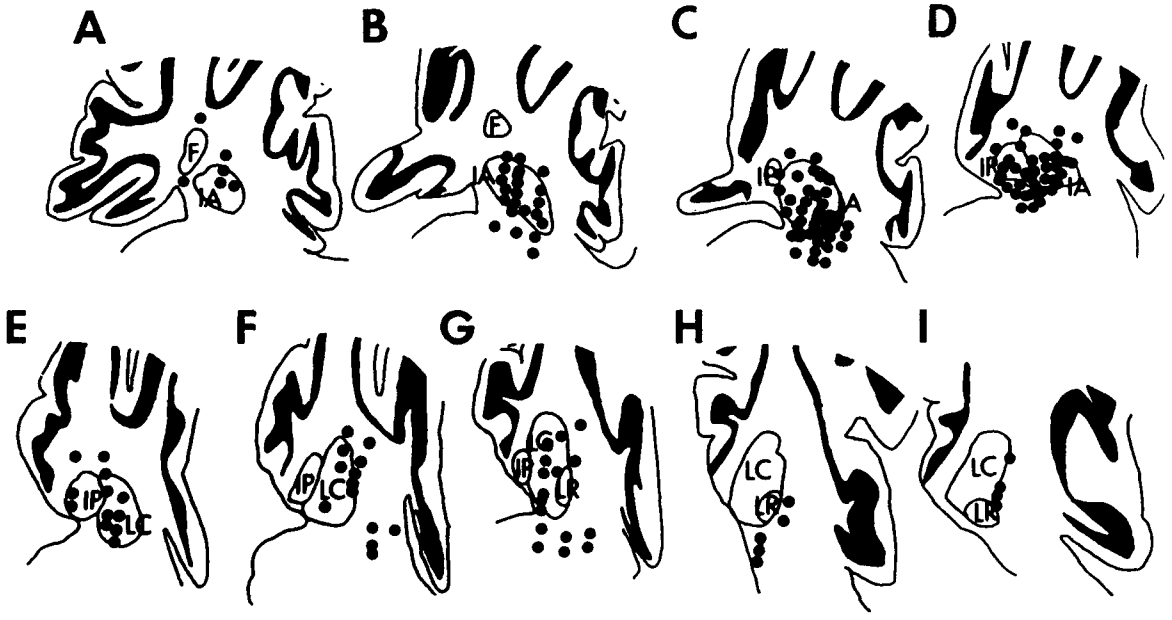

Fig. 2A–I. Recording sites of the 165 deep nuclear and surrounding cells discussed in this paper. Drawings are sequential parasagittal sections at 0.5 mm separation beginning 2 mm from the midline and proceeding laterally. Rostral is to the right. Abbreviations: F: fastigial, IA: anterior interpositus, IP: posterior interpositus, LC: lateral pars convexa, LR: lateral pars rotunda (after Van Rossum 1969)

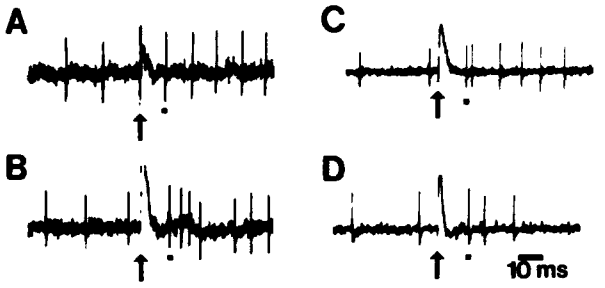

Fig. 3A–D. Response of four deep nuclear cells to the US. The arrows point to US artifact and the filled squares indicate the first evoked spike. These cells responded with latencies of 10 to 13 ms

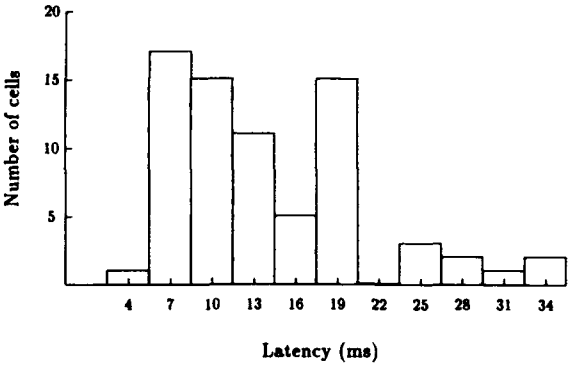

Fig. 4. Response of deep cerebellar cells to periorbital electrical stimulation (US). The majority of cells responded at 6 to 20 ms latency

of the neural response. Nictitating membrane response latencies were also noted. The distribution of neural response latencies is shown in Fig. 4. Figure 4 shows that neural response latency was bimodally distributed with peaks at 7 and 19 ms after US onset. The earliest spike responses were of shorter latency than the earliest NM responses. The mean neural response latency was 14.5 ms (SD = 8.1, range = 4–50 ms), and the mean NM latency was 14.6 ms (SD = 4.3, range = 9–34 ms).

The 77 US-responsive cells could be sorted into two groups on the basis of whether the first response to the US was an increase or a decrease in firing. Fifty-three cells bursted at US onset, and 24 cells slowed or ceased firing when the US was presented. The cells that increased firing to the US did not differ in latency from those that decreased firing to the US (Kolmogorov-Smirnov test).

The effects of the US on ongoing CRs

The effect of the US on NM position was a short-latency (10–20 ms), short-duration (100 ms) extension followed by a retraction to baseline. In those cases where CRs were being made during US application, i.e., on CS+ trials, the effect of the US was to interrupt the CR. The shortening of behavioral CRs was clearly seen during the recording periods of 60 of the 165 cells and is illustrated in Fig. 5. Figure 5A shows CS+ trials on which USs were presented, and Fig. 5B shows CS− trials, most of which containing CRs. Inspection of the two panels reveals that CRs on CS+ trials were of shorter durations than CRs on CS− trials. Thus, whereas US presentation elicited or enhanced NM extension, it was rapidly followed by a return of the NM to its retracted position. By contrast, CRs on CS− trials extended for several hundred milliseconds and returned to baseline slowly. It is clear that the shortening of CRs seen in this case was not artifactually due to the dynamics of the transducer, since neural activity paralleled performance of the CR.

Shortening of the CR was seen during the recording periods of 13 cells that showed both CR and US related activity. In eight of these cells the US produced responses that were opposite in polarity to the activity during the CR.

Short-latency responses to the CSs

For each cell, Kolmogorov-Smirnov tests, averaged over trials of both types were used to compare interspike intervals during the 100 ms preceding CS onset, with interspike intervals during the 100 ms after CS onset. In the event of a significant difference, peristimulus-time rasters and histograms were then inspected to confirm responses to the CSs. Thirty-eight cells showed significant responses to the CSs. However, for three of these cells the response appeared small or inconsistent in rasters and histograms. These three cells were excluded from further analysis. Of the remaining 35 cells, 20 increased firing at CS onset, while 15 slowed or ceased firing at CS onset.

About half of the cells responded to the CSs with latencies less than 20 ms, irrespective of whether cells responded by an increase or decrease in firing. Nineteen cells responded with bursts, while 16 showed responses that lasted for the duration of the CS. Two cells showed much greater modulation to the CS+ than the CS−.

Changes in neural activity during CRs

Kolmogorov-Smirnov tests were used to detect changes in firing associated with CRs. This was done by comparing firing during a period 150 ms before to 50 ms after CR onset with pre-CS baseline. Eighty-one cells showed significant changes in firing by this criterion. However, seven of these cells showed significant changes only because the neural response started at CS onset and continued until CS offset. The responses of these seven cells were considered to be auditory responses, and they were excluded from further analysis. Data were excluded from six other cells because of high variability in firing patterns or because the data were obtained from less than three trials. The remaining 68 cells were classified as CR-related.

The lead-time of the neural response with respect to CR onset was estimated from cumulative sums of peri-CR time histograms. The lead times of three cells could not be

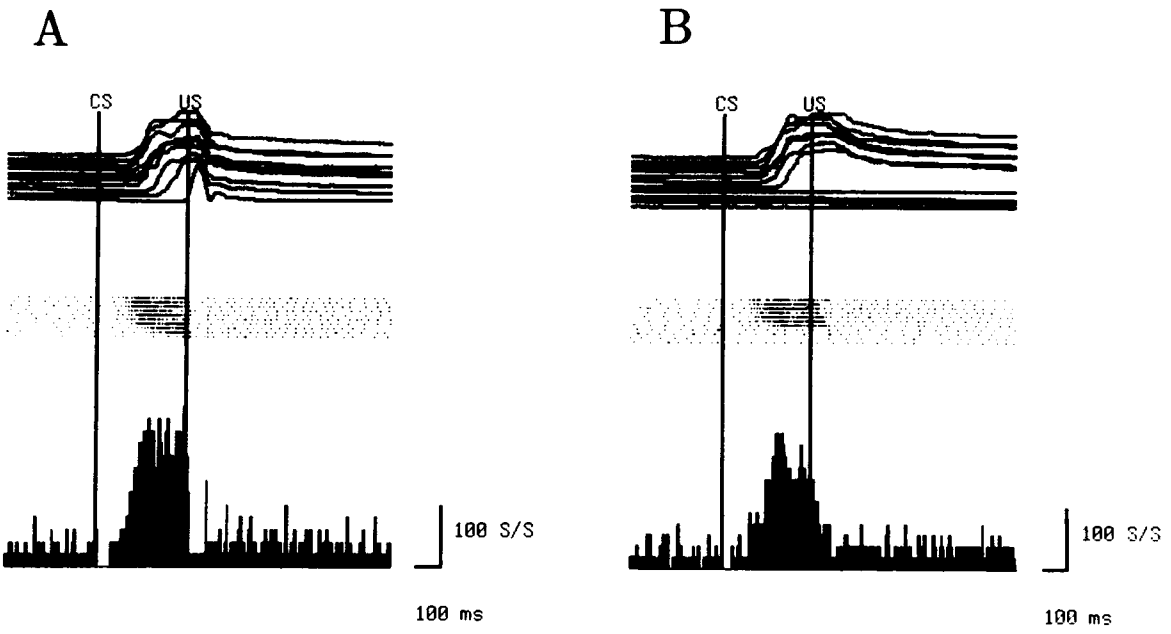

Fig. 5A, B. The effect of the US on CRs. Panel **A** shows the activity of a cell on CS+ trials and panel **B** the activity on CS− trials. The vertical lines through each panel indicate CS and US onset (the vertical line in panel **B** shows the time at which the US was presented on CS+ trials; no USs were given on CS− trials). The top section of each panel shows NM position traces, the middle section shows rasters of spike activity in the same order as the NM traces, and the bottom shows a histogram of spike activity. Bin width = 5 ms

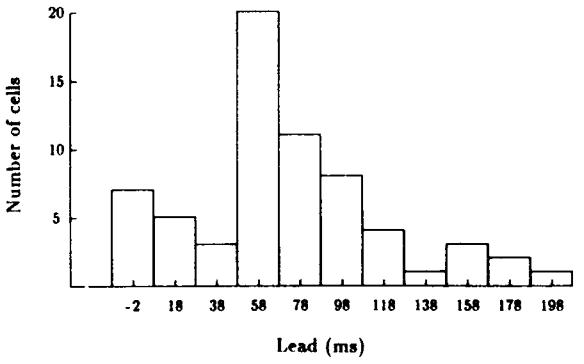

Fig. 6. The neural response lead of NM movement for deep nuclear cells estimated from cumulative sums of peri-CR time histograms. Negative times indicate that the neural response lagged CR onset

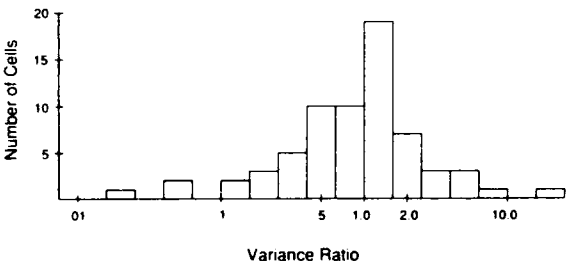

Fig. 7. A frequency histogram of the VRs. The VRs are plotted on a logarithmic scale since the VRs are a ratio. For example, a VR of 0.1 or 10 means that one variance was ten times the magnitude of the other variance

determined because of the small amplitude of the neural response relative to baseline. For the remaining cells (N = 65) the times ranged from 191 ms to −12 ms, with a mean of 71.4 ms (SD = 46.0) and a median of 64 ms. A histogram of the lead-times for these 65 cells is presented in Fig. 6.

The lead-times were similar for cells that increased or decreased firing on CR trials. The lead-times for cells that increased firing on CR trials (N = 49) ranged from 191 ms to −12 ms, with a mean of 72.1 ms (SD = 46.3) and a median of 64 ms. The lead-times for the cells that decreased firing on CR trials (N = 16) ranged from 170 ms to −10 ms, with a mean of 68.9 ms (SD = 49.0) and a median of 68 ms.

Neural firing change-points related to variations in CR latency

Variance ratios were computed for the CR-related cells to determine how neural activity shifted as CR latency varied from trial to trial. Conditioned response onset and firing change-point latencies were obtained for 64 of the 68 CR-related cells. Four of these cells had two firing change-points per trial that could be differentiated with our algorithm. Variance ratios were computed for these 68 neural responses and their distribution is shown in Fig. 7.

Thirty-three VRs were less than one indicating that the neural responses were movement related. Thirty-five VRs were greater than one indicating that the neural responses were stimulus related. Sixteen VRs were less than 0.5, and 12 were greater than two (two of the 12 ratios greater than two were from the same cell). The recording sites for these 27 cells with the most extreme VRs are shown in Fig. 8. An example of a stimulus related interpositus cell (52a) is shown in Fig. 9. This neuron decreased its firing on trials on which CRs were made. This cell's VR was 3.39. The decrease in firing was time-locked to CS onset and was seen only on trials with CRs.

An example of a movement related NIA cell (48c) is shown in Fig. 10. This cell's activity increased on CR trials. No movement correlated activity was seen on trials without CRs. The change in activity led CRs by about 75 ms (value determined from peri-CR histogram). The VR for this cell was 0.48 indicating that the neural response shifted with shifts in CR latency.

Figures 9 and 10 also show that CR-related cells typically responded to the CS and US. The cell shown in Fig. 9 shows increased responding about the time of US-onset, and the cell shown in Fig. 10 increased responding at CS-and US-onset.

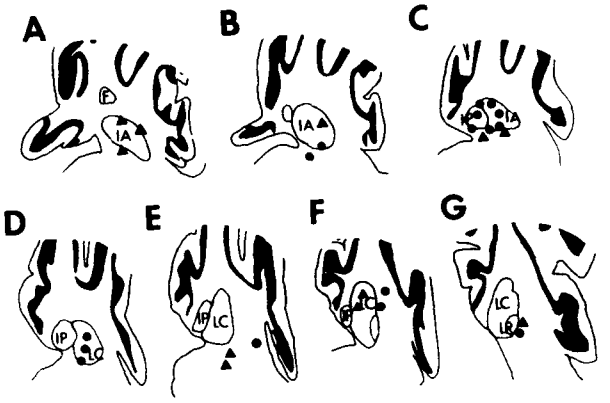

Fig. 8A–G. Recording sites for 16 cells that showed marked movement related activity (circles) and 11 cells that showed marked stimulus related activity (triangles; one cell had two ratios computed for a total of 12 ratios). Drawings are sequential parasagittal sections at 0.5 mm separation starting at 2.5 mm from the midline and proceeding laterally. Abbreviation as in Fig 2

Combinations of US, CS, and CR responses

Figure 11 shows the various combinations of patterns of responses to the US, CSs, and CR in the form of a Venn diagram. Cells were partitioned on the basis of whether they responded to the US, CSs, and whether they were CR-related. Table 1 shows a more complete summary of Fig. 11 showing the direction or polarity of neural responses to trial events.

CR-related cells were equally likely to respond to the US (37/68, 54%) as non CR-related cells (41/97, 42%; $\chi^2 = 1.42$, $p > 0.05$). However, CR-related cells were more

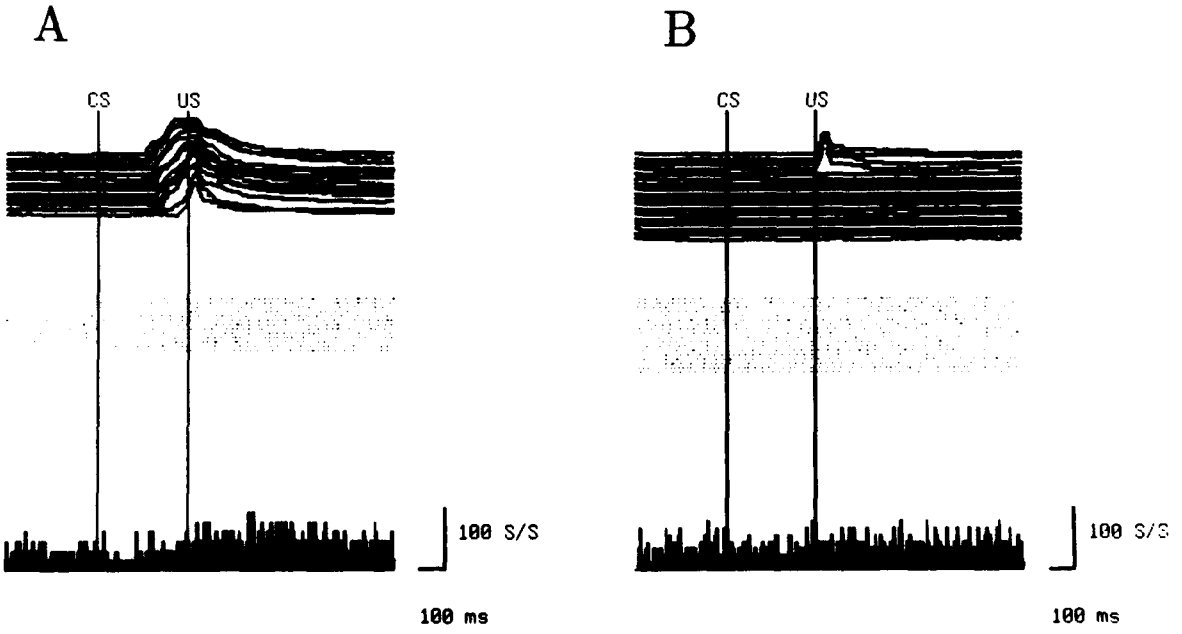

Fig. 9A, B. A cell (52a) that showed CR-related decrease in firing timed to CS onset. Panel A shows data from trials on which CRs occurred and panel B shows data from trials on which CRs did not occur. The vertical lines show the times of CS and US onset. (The US was presented only on those trials in panels A and B that were CS+ trials.) The top section of each panel shows NM position traces, the middle shows rasters arranged in the same order as the NM traces, and the bottom shows a histogram of neural activity. The position traces and rasters are presented from top to bottom in order of CR latency

Table 1. Polarity of neural response for each combination of patterns to trial events

1. Responded to one of the events:
   Responded to tone: 4 increased firing and 5 decreased firing
   Responded to US: 26 increased firing and 11 decreased firing
   Responded on CR trials: 16 increased firing and 5 decreased firing
2. Responded to two of the events:
   Responded to tone and US: 2 increased firing to both, 1 increased to the tone and decreased to the US, 1 increased to the US and decreased to tone.
   Responded to tone and on CR trials: 6 increased to both, 1 increased to tone and decreased to CR, 3 decreased to tone and increased to CR
   Responded to US and on CR trials: 11 increased to both, 4 increased to CR and decreased to US, 6 decreased to CR and increased to US, and 4 decreased to both
3. Responded to all three events:
   Responded to US by increase in firing: 4 increased to CR and tone, 2 increased to CR and decreased to tone, 1 increased to the tone and decreased to the CR, and 1 decreased to both
   Responded to US by decrease in firing: 2 increased to CR and tone, 2 increased to CR and decreased to tone

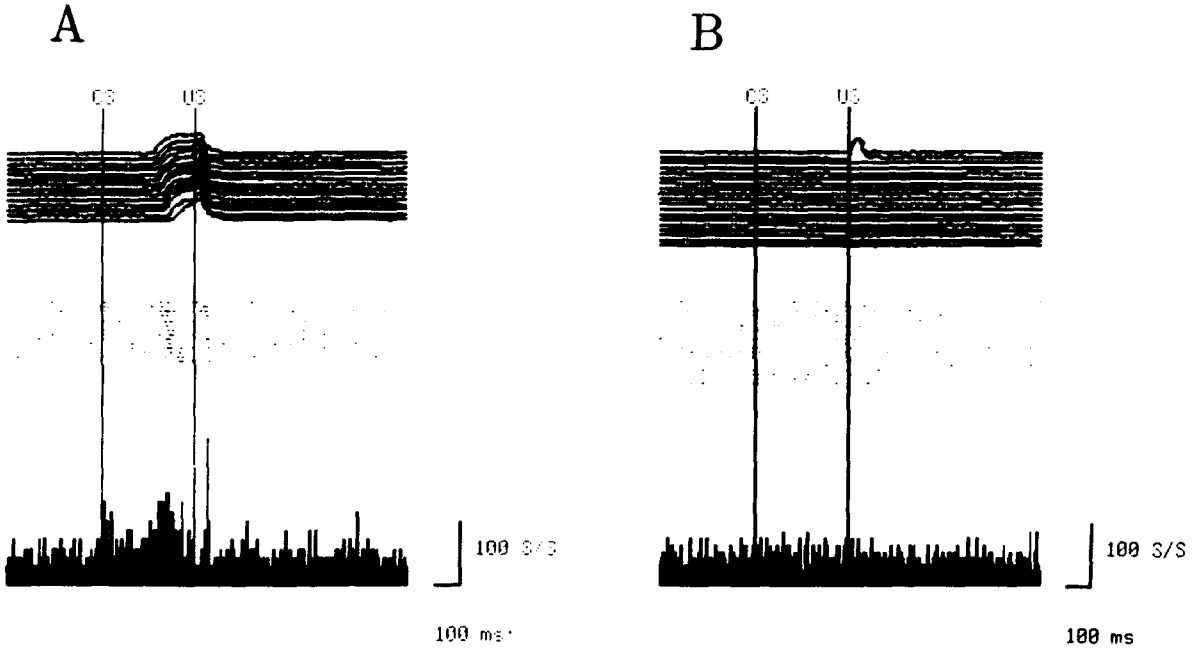

Fig. 10A, B. A cell (48c) that showed movement related firing. Data presented as in Fig. 9

likely to respond to the CSs (22/68, 33%) than non CR-related cells (13/97, 14%; $\chi^2 = 8.61$, $p \leq 0.05$). CR-related cells were also more likely to respond to both the CSs and US (12/68, 17%) than non CR-related cells (4/97, 4%; $\chi^2 = 6.88$, $p \leq 0.05$). Similar χ^2-tests failed to show significant differences between stimulus and movement related cells in responsiveness to the CSs or US.

One prediction that a simple stimulus substitution view of classical conditioning makes is that the direction of modulation (i.e., whether firing increases or decreases) of a cell during a CR should be the same as the direction of modulation to the US. In the present study cells that showed movement related activity were about equally likely to modulate in opposite as in the same direction. Out of 19 cells that were movement related and showed US-evoked activity, 10 modulated in opposite directions during the CR and US.

Discussion

The present investigation demonstrates that cerebellar deep nuclear cells respond to the US and CSs used in classical eye blink/NM conditioning. Forty-seven percent of the cells showed responses to the stimulation of the periorbital area used as the US. Unconditioned stimulus-evoked responses varied in latency from 5.5 to about 30 ms, with most cells responding within 15 ms. Twenty-four percent of the cells showed short latency responses to CS onset. These responses were typically seen to both the CS+ and CS−. Neural responses evoked by CSs were either a burst of spikes to CS onset or a tonic response that persisted for the duration of the CS. Forty-one percent of the cells were labelled CR-related since they fired when CRs were made. CR-related changes in firing led CR onset by an average of 71 ms. About half of the CR-related cells

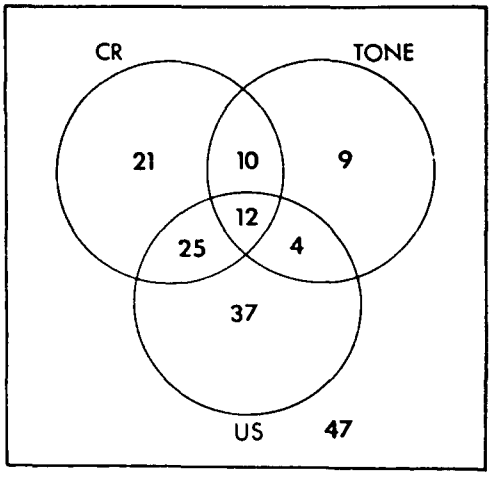

Fig. 11. Venn diagram of combinations of responses to the US, CS (tone), and CR

were movement related since their firing followed variations of CR latency.

Neural responses to the US

The response of cells to the US is mediated by the trigeminal system, which conveys somatosensory information from the orbital area of the face. Trigeminal mossy fibers project to the cerebellum by three pathways. The first pathway is a direct projection from the trigeminal nerve. Jacquin et al. (1982) found labeled mossy fibers in Crus I and II, paramedian lobule, and dentate after HRP injection in the trigeminal ganglion. A second pathway is via the trigeminal complex. Ikeda (1979), Mantle-St. John and Tracey (1987), and Silverman and Kruger (1985) demonstrated labeling of oralis, interpolaris, caudalis, and principal sensory neurons after injections of retrograde tracers into lobules V and VI, and Crus I and II. Trigeminal neurons that project to the cerebellum do not send collaterals to the thalamus or tectum (Silverman and Kruger, 1985). A third projection from the trigeminal complex to the cerebellar cortex and NIA is via the lateral reticular nucleus (Dietrichs and Walberg 1987; McCrea et al. 1977).

Climbing fibers also carry facial somatosensory information. Walberg (1982) showed that all divisions of the trigeminal complex, except the principal sensory and mesencephalic nuclei, project contralaterally to the inferior olive. Courville et al. (1983) concluded that the major trigeminal projection to the inferior olive arises from pars interpolaris and caudalis and that the projection from pars oralis is sparse. The inferior olive projects to cerebellar cortex as well as the deep cerebellar nuclei (Dietrichs and Walberg 1986; Van der Want et al. 1989; Yeo et al. 1985).

The US responses seen in the present study could be the result of direct input from climbing or mossy collateral input or indirect input from cortical Purkinje cells. Darian-Smith et al. (1964) showed that trigeminal neurons respond to stimulation of their facial receptive fields with a latency of 3 ms. Lobule VI granule cells respond with a latency of 4 to 5 ms (Kassel et al. 1984), and lobule VI Purkinje cells respond with a latency of 5 to 8 ms to facial stimulation (Cody and Richardson 1979). These values are consistent with Woolston et al. (1981) who found a 1.3-ms conduction time from interpolaris to cerebellar cortex. Cody and Richardson (1979) found that climbing fiber responses in cerebellar cortex were elicited with 9 to 35 ms latency to stimulation of the face. Given these values, a direct trigemino-deep nuclear projection would have a latency of less than 5 ms. Since the shortest US-elicited response observed in the present study was 5.5 ms, a direct trigemino-deep cerebellar nuclear pathway probably would not be involved in US-elicited neural responses. However, many of the US-elicited responses must have been mediated by mossy fibers because many deep cerebellar nuclei cells discharged before climbing fibers could become active.

In many cases the US decreased the duration of the behavioral CR and CR-related firing. This suggests that periorbital stimulation might serve to terminate CRs as well as serving as a US. It may be that the eye blink is controlled by two systems: a trigemino-motoneuronal system involved in unconditioned blinks and a cerebellar system controlling or modulating the CR. In the present preparation the US may modulate the CR-producing system so that the CR-producing system does not interfere with UR production.

Neural responses to CSs

One hypothesis of the cerebellum's role in classical conditioning is that it is the site of learning. Theories such as those of Marr (1969) and Albus (1971) contend that the cerebellum is a site where a CS is associated with a US. In these theories the CS and US converge onto Purkinje cells to produce the CR. While the present experiment was not designed to investigate the auditory responsiveness of the deep cerebellar nuclei, the results indicate that some deep cerebellar neurons show time-locked responses to the CSs. Some of these responses are seen only when CRs are made, and others are seen independent of CRs. The CS-locked responses that are independent of CR performance are probably sensory responses to the auditory stimuli.

Aitkin and Boyd (1975), Freeman (1970), and Huang and Burkard (1986) confirm that the cerebellum receives auditory inputs. These responses are widely tuned with most cells responding to tones phasically, although some tonic responses are seen (Aitkin and Boyd 1975; Huang and Burkard 1986). The responses seen in these auditory studies are similar to the responses seen in conditioning studies using auditory CSs. Berthier and Moore (1986) found that Purkinje cells respond similarly to auditory CSs differing in frequency by about half an octave. In the present experiment we found that deep nuclear cells respond similarly to the two tones used as CSs. About half of the cells showed phasic responses and half showed tonic responses.

The auditory input to the cerebellum originates in the inferior colliculus and cerebral cortical area AII and projects via the dorsolateral pontine nuclei (DLPN) to the cerebellar cortex (Huang and Burkard 1986). Recordings from DLPN confirm that DLPN neurons show broad tuning curves (Aitkin and Boyd 1978). A direct pathway from the cochlear nuclei to cerebellar cortex has also been described (Huang et al. 1982).

One problem for theories of cerebellar learning is that recordings of cerebellar afferents suggest that auditory inputs do not contain specific frequency information. If the Marr-Albus theories are correct, how can auditory differential conditioning occur in the cerebellum if afferents respond similarly to both the CS+ and CS−? It is possible that sensory information underlying a behavioral discrimination might reach the cerebellum through one of the anatomically demonstrated, but yet to be physiologically studied, pathways, e.g., the direct pathway from the cochlear nuclei to cerebellar cortex (Huang et al. 1982). Alternatively, the pathways already studied might utilize coarse codes that would allow Purkinje cells to extract specific frequency information at the level of the parallel fiber-Purkinje cell synapse.

The effect of shifts in CR latency on deep nuclear activity

In the present study about half of the cells that showed CR-related activity showed movement related firing, and about half showed stimulus related firing. The change in firing of the most movement related cells led the CR by about 60 ms. The timing of CR correlated activity seen in the present study was very similar to that of Chapman et al. (1986) who analyzed the activity of deep cerebellar nuclear cells during learned arm movements in monkey to visual, auditory, and somesthetic stimuli. Chapman et al. (1986) concluded that stimulus related cells are involved in triggering or initiating the movement and that movement related cells are involved in controlling the execution of the movement. Movement related cells recorded in the present study are also candidates for the production and control of the NM CR. These cells led the behavior by a sufficient amount of time to be causal and are highly predictive of its occurrence.

Conclusions

In sum, lesion and anatomical studies suggest that the cerebellum is involved in learning of the eye blink/NM CR (e.g., McCormick et al. 1982b; Yeo et al. 1985b). Electrophysiological studies show that the cerebellum receives convergent information about the CSs and USs used in classical conditioning (Berthier and Moore 1986; Foy and Thompson 1986). This evidence has been cited to support the hypothesis of Marr (1969) and Albus (1971) that associative motor learning occurs within the cerebellum (see also, Ito 1984). The present study extends these results by showing that the firing of some deep nuclear neurons was highly correlated with the performance of the CR. In addition, many of the deep nuclear cells that responded during CRs also responded to the CSs and US. Taken as a whole, the evidence suggests that CRs are formed and generated within the cerebellum. However, most deep cerebellar nuclear neurons in the present study showed short latency auditory responses that did not discriminate between the CS− and CS+, a result that is consistent with other studies that show that the cerebellum receives only broadband auditory inputs (e.g., Aitkin and Boyd 1975). This broadband tuning would imply that mechanisms whereby CRs are suppressed to a CS− which is psychophysically similar to the CS+ involve systems extrinsic to the cerebellum.

Acknowledgements. The authors are indebted to Dr. J.E. Desmond for his comments on the manuscript. Supported by AFOSR 89-0391 and NSF BNS 88-10624.

References

Aitkin LM, Boyd J (1975) Responses of single units in cerebellar vermis of the cat to monaural and binaural stimuli. J Neurophysiol 38: 418–429

Aitkin LM, Boyd J (1978) Acoustic input to the lateral pontine nuclei. Hearing Res 1: 67–77

Albus JS (1971) A theory of cerebellar function. Math Biosci 10: 25–61

Armstrong DM, Edgley SA (1984) Discharges of nucleus interpositus neurones during locomotion in the cat. J Physiol (Lond) 351: 411–432

Berthier NE, Moore JW (1986) Cerebellar Purkinje cell activity related to the classically conditioned nictitating membrane response. Exp Brain Res 63: 341–350

Billard JM, Batini C, Daniel H (1988) The red nucleus activity in rats deprived of the inferior olivary complex. Behav Brain Res 28: 127–130

Chapman CE, Spidalieri G, Lamarre Y (1986) Activity of dentate neurons during arm movements triggered by visual, auditory and somesthetic stimuli in the monkey. J Neurophysiol 55: 203–226

Cody F, Moore RB, Richardson HC (1981) Patterns of activity evoked in cerebellar interpositus nucleus neurons by natural somatosensory stimuli in awake cats. J Physiol (Lond) 317: 1–20

Cody FWJ, Richardson HC (1979) Mossy and climbing fibre mediated responses evoked in the cerebellar cortex of the cat by trigeminal afferent stimulation. J Physiol (Lond) 287: 1–14

Commenges D, Seal J (1986) The formulae-relating slopes, correlation coefficeints and variance ratios used to determine stimulus- or movement-related neuronal activity. Brain Res 383: 350–352

Courville J, Faraco-Cantin F, Marcon L (1983) Projections from the reticular formation of the medulla, the spinal trigeminal and lateral reticular nuclei to the inferior olive. Neuroscience 9: 129–139

Darian-Smith I, Proctor R, Ryan RD (1964) A single-neurone investigation of somatotopic organization within the cat's trigeminal brain-stem nuclei. J Physiol (Lond) 168: 147–157

Dietrichs E, Walberg F (1986) The cerebellar nucleo-olivary and olivocerebellar nuclear projections in the cat as studied with anterograde and retrograde transport in the same animal after implantation of crystalline WGA-HRP. III. The interposed nuclei. Brain Res 373: 373–383

Dietrichs E, Walberg F (1987) Cerebellar nuclear afferents where do they originate? A re-evaluation of the projections from some lower brain stem nuclei. Anat Embryol 177: 165–172

Desmond JE, Moore JW (1987) Red nucleus single-unit activity during the classically conditioned rabbit nictitating membrane response. Soc Neurosci Abstr 13: 841

Evinger C, Manning KA (1988) A model system for motor learning: adaptive gain control of the blink reflex. Exp Brain Res 70: 527–538

Foy MR, Thompson RF (1986) Single unit analysis of Purkinje cell discharge in classically conditioned and untrained rabbits. Soc Neurosci Abstr 12: 518

Freeman JA (1970) Responses of cat cerebellar Purkinje cells to convergent inputs from cerebral cortex and peripheral sensory systems. J Neurophysiol 33: 697–712

Huang C, Burkard R (1986) Frequency sensitivities of auditory neurons in the cerebellum of the cat. Brain Res 371: 101–108

Huang CM, Liu G, Huang R (1982) Projections from the cochlear nucleus to the cerebellum. Brain Res 244: 1–8

Ikeda M (1979) Projections from the spinal and the principal sensory nuclei of the trigeminal nerve to the cerebellar cortex in the cat, as studied by retrograde transport of horseradish peroxidase. J Comp Neurol 184: 567–586

Ito M (1984) The cerebellum and neural control. Raven Press, New York

Jacquin MF, Semba K, Rhoades RW, Egger MD (1982) Trigeminal primary afferents project bilaterally to dorsal horn and ipsilaterally to cerebellum, reticular formation, and cuneate, solitary, supratrigeminal, and vagal nuclei. Brain Res 246: 285–291

Kassel J, Shambes G, Welker W (1984) Fractured cutaneous projections to the granule cell layer of the posterior cerebellar hemisphere of the domestic cat. J Comp Neurol 225: 458–468

Lamarre Y, Busby L, Spidalieri G (1983) Fast ballistic arm movements triggered by visual, auditory and somesthetic stimuli in the monkey. I. Activity of precentral cortical neurons. J Neurophysiol 50: 1343–1358

Lavond DG, Steinmetz JE, Yokaitis MH, Thompson RF (1987) Reacquisition of classical conditioning after removal of cerebellar cortex. Exp Brain Res 67: 569–593

Lisberger SG (1988) The neural basis for learning simple motor skills. Science 242: 728–735

Mantle-St. John LA, Tracey DJ (1987) Somatosensory nuclei in the brainstem of the rat: independent projections to the thalamus and cerebellum. J Comp Neurol 255: 259–271

Marr D (1969) A theory of cerebellar cortex. J Physiol (Lond) 202: 437–470

Marr D, Hildreth E (1980) Theory of edge detection. Proc R Soc Lond (B) 207: 187–217

McCormick DA, Clark GA, Lavond DG, Thompson RF (1982a) Initial localization of the memory trace for a basic form of learning. Proc Natl Acad Sci (USA) 79: 2731–2735

McCormick DA, Guyer PE, Thompson RF (1982b) Superior cerebellar peduncle lesions selectively abolish the ipsilateral classically conditioned nictitating membrane/eyelid response of the rabbit. Brain Res 244: 347–350

McCormick DA, Lavond DG, Thompson RF (1982c) Concomitant classical conditioning of the rabbit nictitating membrane and eyelid responses: correlations and implications. Physiol Behav 28: 769–775

McCormick DA, Thompson RF (1984) Neuronal responses of the rabbit cerebellum during acquisition and performance of a classically conditioned nictitating membrane-eyelid response. J Neurosci 4: 2811–2822

McCrea RA, Bishop GA, Kitai ST (1977) Electrophysiological and horseradish peroxidase studies of precerebellar afferents to the nucleus interpositus anterior. II. Mossy fiber system. Brain Res 122: 215–228

Miles FA, Fuller JH, Braitman DJ, Dow BM (1980) Long-term adaptive changes in primate vestibuloocular reflex. III. Electrophysiological observations in flocculus of normal monkeys. J Neurophysiol 43: 1437–1476

Moore JW, Berthier NE (1987) Purkinje cell activity and the conditioned nictitating membrane response. In: Glickstein M, Yeo C, Stein J (eds) Cerebellum and neuronal plasticity. Plenum, New York, pp 339–352

Rosenfield ME, Moore JW (1983) Red nucleus lesions disrupt the classically conditioned nictitating membrane response in rabbits. Behav Brain Res 10: 393–398

Silverman JD, Kruger L (1985) Projections of the rat trigeminal sensory nuclear complex demonstrated by multiple flourescent dye retrograde transport. Brain Res 361: 383–388

Strata P (1985) Inferior olive: functional aspects. In: Bloedel JR, Dichgans J, Precht W (eds) Cerebellar functions. Springer, Berlin, pp 230–246

Thompson RF (1986) The neurobiology of learning and memory. Science 233: 941–947

Tsukahara N, Oda Y, Notsu T (1981) Classical conditioning mediated by the red nucleus in the cat. J Neurosci 1: 72–79

Türker KS, Miles TS (1986) Climbing fiber lesions disrupt conditioning of the nictitating membrane response in the rabbit. Brain Res 363: 376–378

Van Rossum J (1969) Corticonuclear and corticovestibular projections of the cerebellum. Ph.D. thesis. University of Leiden

Van der Want JJL, Wicklund L, Guegan M, Ruigrok T, Voogd J (1989) Anterograde tracing of the rat olivocerebellar system with Phaseolus vulgaris leucoagglutinin (PHA-L): demonstration of climbing fiber collateral innervation of the cerebellar nuclei. J Comp Neurol 288: 1–18

Walberg F (1982) Trigemino-olivary projection in the cat studied with retrograde transport of horseradish peroxidase. Exp Brain Res 45: 101–107

Woolston DC, Kassel J, Gibson JM (1981) Trigeminocerebellar mossy fiber branching to granule cell layer patches in the rat cerebellum. Brain Res 209: 255–269

Yeo CH, Hardiman MJ, Glickstein M (1985a) Classical conditioning of the nictitating membrane response of the rabbit I. Lesions of the cerebellar nuclei. Exp Brain Res 60: 87–98

Yeo CH, Hardiman MJ, Glickstein M (1985b) Classical conditioning of the nictitating membrane response of the rabbit. II. Lesions of the cerebellar cortex. Exp Brain Res 60: 99–113

Yeo CH, Hardiman MJ, Glickstein M (1986) Classical conditioning of the nictitating membrane response of the rabbit. IV. Lesions of the inferior olive. Exp Brain Res 63: 81–92

NEURAL NETWORK MODELS OF CONDITIONING AND ACTION

A Volume in the Quantitative Analyses of Behavior Series

Edited by

MICHAEL L. COMMONS
Harvard Medical School

STEPHEN GROSSBERG
Boston University

JOHN E. R. STADDON
Duke University

LEA LAWRENCE ERLBAUM ASSOCIATES, PUBLISHERS
1991 Hillsdale, New Jersey Hove and London

7 Implementing Connectionist Algorithms for Classical Conditioning in the Brain

John W. Moore
University of Massachusetts

ABSTRACT

Simple connectionist models of learning that conform to the Widrow-Hoff rule can be parameterized and extended to describe real-time features of classical conditioning. These features include the dependence of learning on the moment-to-moment status of input to the computational system and on the desired topography of its output. Using the classically conditioned nictitating response (NMR) of the rabbit as a prototypal system, my coworkers and I have devised models that successfully meet these real-time criteria. Two models and neural network architectures are described. The first consists of a single neuron-like processor with learning rules based on the Sutton-Barto model. The second consists of two neuron-like units with input based on a tapped-delay line representation of stimuli. Using anatomical and physiological data,both network models can be aligned with brain stem and cerebellar circuits involved in classical NMR conditioning. These models and their implementation in the brain have testable empirical consequences.

This chapter illustrates how computational models based on abstract neural networks can provide insights into questions such as where in the brain learning occurs and the mechanisms that bring it about. It serves as a tutorial on aligning quantitative learning theory with physiology, thereby establishing a potential conduit for communication between molar and molecular levels of analyses. One might say that such efforts are about bringing abstract models to life in real nervous systems. Specifically, it brings together two lines of research: (a) studies of brain circuits underlying classical conditioning of a simple skeletal response, the rabbit nictitating membrane response (NMR) and (b) developing computational models applicable to real-time conditioning phenomena such as response

topography and CS-US interval effects. Our work stands on a foundation provided by the "extended laboratory" (Gabriel, 1988) of those who investigate classical eye blink/NMR conditioning (Gormezano, Prokasy, & Thompson, 1987).

This chapter also illustrates Churchland's (1986) point that a theoretical dimension can be added to the neurosciences through a process of coevolution. Theories, expressed as computational algorithms, can guide decisions about where best to invest experimental resources. Behavioral neuroscientists regard the preparations they investigate as model systems, and therefore they are not indifferent to the broader implications of their work. However, they believe that exploiting these implications requires understanding the model system at multiple levels. At the computational level, this understanding is expressed in terms of algorithms capable of simulating how the system behaves under a range of environmental challenges. Production systems have this capability. More interesting and useful in the long run are algorithms that *emulate* what actually occurs in the brain to cause the system to behave as it does.

I shall recount some of the steps my colleagues and I have taken in evaluating models of classical conditioning and casting them in terms of neural networks that might convincingly be implemented in real brains. By this I refer to discovering *alignments* between models and what is known of the anatomy and physiology underlying a given CR. I say "a given CR" because we are concerned primarily with developing theoretical frameworks useful to neuroscientists. As neuroscientists, our interest in theory cannot stray very far from the nuts and bolts of our experimental work. As neuroscientists, workers in the extended NMR conditioning laboratory seek a deep understanding of classical conditioning. Such an understanding demands rigorous theoretical expression, and thus NMR conditioning has been approached from three directions—behavior, biology, and computation. The overriding objective is to integrate these approaches in much the same way that oculomotor physiologists have done with saccadic eye movement and vestibular oculomotor reflexes (Robinson, 1981, 1989). The oculomotor example is apt because of shared anatomical systems.

Before proceeding, some comment about the title is in order. The title speaks of *implementing* connectionist algorithms[1] in the brain. Others have applied the term *instantiation* to this process. When considering the dictionary definitions of these two terms, I find implementation more apt. According to *Webster's New Collegiate Dictionary*, the infinitive "to instantiate" means "to represent an abstraction by a concrete example" whereas "to implement" means "to provide instruments or means of expression."

I would argue that instantiation is a prerequisite to implementation. To illustrate, my colleagues and I began by selecting one abstract computational theory, the Sutton-Barto (SB) model, which showed promise in describing many of the basic phenomena of classical conditioning, particularly the molar features of classical conditioning of the eye blink/NMR (Barto & Sutton, 1982; Sutton & Barto, 1981). We then sought a specific *instance* of the SB model that could describe in detail real-time features of the conditioned NMR, including response topography. We have referred to the resulting constrained and parameterized version of the model as the Sutton-Barto-Desmond (SBD) model (Moore et al., 1986). By common usage,the SBD model is an *instantiation*—a concrete representation—of the abstract SB model. When we speak of implementing this model (Moore & Blazis, 1989a, 1989b, 1989c), we mean finding brain processes and mechanisms ("instruments") conceivably capable of generating and explaining the measurable consequences of its parameterized and algorithmic ("instantiated") form.

Animal learning theorists are accustomed to evaluating models solely by behavioral criteria. They also prefer models that are parsimonious and elegant. Difficulties arise when there are many serviceable models to account for phenomena at the level of behavior. The instantiation of models into algorithmic and parameterized form adds constraints to models that are useful in their evaluation, but even at this level of exactness the choice of the more valid model can be arbitrary. Animal learning theorists attempt to escape from this dilemma by designing elaborate experiments that test highly refined behavioral predictions. Although not minimizing the importance of this strategy, I suggest that a brain implementation scheme can imply independent experimental assessments of models using criteria at the level of neurobiology as an adjunct to behavioral criteria. It goes without saying that the success of this approach depends on having accurate information about neural substrates of the behavior being modeled. Implementation schemes should be physiologically compelling, not merely plausible. Later on I illustrate this point by showing how implementation schemes my colleagues and I have devised for two models have testable hypotheses in the domain of neurophysiology. The situation is somewhat comparable to neuroanatomists' quest for Renhaw cells, which was stimulated by physiologists' claims that they must exist.

Devising good implementation schemes for instances of mammalian behavior such as NMR conditioning is not easy. It is difficult because of the virtual impossibility of obtaining direct and rigorous proof that mechanisms proposed to account for phenomenology actually exist and function in ways consistent with the model. We must therefore approach the question of mechanisms indirectly through experimental probes—testing behavioral predictions, making lesions or pharmacologic interventions, and recording neural activity. It would be comforting if agreed-upon facts were not open to differing interpretation, but this state of affairs seldom exists. However, it is more important to *identify* agreed-upon

[1] Connectionist algorithms refer to any member of a class of models cast in terms of modifiable connection weights among neuron-like processing elements. The term is not limited to the so-called delta or LMS learning rule or to learning through back-propagated error correction.

experimental evidence than to seek consensus on what the evidence means. What, then, of experimental facts that are in dispute, and which disputes are most crucial to resolve? A good model and implementation scheme should tell us.

NEUROBIOLOGICAL BACKGROUND

Much of the difficulty in addressing questions of loci and mechanisms of learning arises from a reliance on lesion data and other indirect evidence. Although lesion data are vitally important, they have left workers in this field with some puzzles that will not be easily resolved. These unresolved issues are important for implementing neural network models of NMR conditioning in the brain. Before considering them, let us review the facts that I believe are *not* in dispute.[2]

- Telencephalic brain regions and structures are not essential for acquisition, maintenance, or performance of the CR. Telencephalic regions that have been the focus of lesion studies include neocortex, hippocampal formation and other components of Papez circuit, basal ganglia, thalamus, and hypothalamus. At the midbrain level, lesion studies have shown that tectum, tegmental reticular formation, substantia nigra, and periacqueductal grey, to mention a few involved structures, are not essential for conditioning. The only essential midbrain structure identified to date is red nucleus (RN).

- Metencephalic brain regions, the cerebellum and brain stem, are essential for the acquisition, maintenance, and performance of CRs. Within the metencephalon, researchers agree that the following subset of structures are essential for expression of *robust* CRs with normal topography: (a) Cerebellar cortex, specifically the region designated by anatomists as hemispheral lobulus VI (HVI); (b) cerebellar nucleus interpositus, specifically the anterior region (NIA); (c) magnocellular RN, specifically the portion that represents the facial region around the eye; (d) inferior olivary nucleus; specifically the dorsal accessory olive (DAO), which represents the facial regions around the eye and sends climbing fibers to HVI and NIA.

- Lesions that disrupt or eliminate CRs in one eye need not affect acquisition or performance of CRs by the other eye. Nor do such lesions interfere with the normal savings of trials to criterion when the US is no longer applied to the affected eye but is switched to the other eye. Since savings can be demonstrated, it is clearly the case that lesions do not impair some general capacity to acquire and store information.

- To a surprising degree, lesions that disrupt or eliminate CRs do not affect the UR, although there may be small modulations of UR amplitude that are understandable in light of known anatomy and physiology.

- The reflex pathways mediating the CR and UR involve motoneurons that innervate the extraocular muscles, especially the retractor bulbi muscles. Most retractor bulbi motoneurons lie in the accessory abducens nucleus (AAN) and are innervated by nearby second-order sensory neurons of spinal trigeminal subnucleus pars oralis (SpoV). Although the brain stem components of these circuits have been well characterized both anatomically and physiologically, the nature and extent of the cerebellum's contribution remains an active area of research. There is strong evidence, outlined later, that the cerebellum makes a substantial *causal* contribution to the generation of CRs.

[2] Space limitations preclude reference to all of the experimental literature bearing on neurobiological substrates of NMR conditioning. Most of the relevant literature can be gleaned from sources such as Gormezano et al., (1987), Moore (1979), Steinmetz, Lavond, and Thompson (1989), and Yeo (1989).

Workers in the extended laboratory of the conditioned NMR have proposed various tests to determine whether CR-disrupting lesions or pharmacologic interventions involving critical metencephalic structures affect learning or performance. CR-disruption might be due to any number of factors unrelated to learning—these might all be subsumed under the heading "performance factors": (a) motor deficit, (b) sensory deficit, (c) disruption of timing, (d) attentional deficit. Motor deficits can be eliminated as a cause of CR disruption to the extent that the UR remains unaffected (over a range of US intensities). Sensory deficits can be eliminated to the extent that CRs are disrupted with different CS modalities. Attentional deficits can be ruled out to the extent that CRs occur in the contralateral eye. Disruptions of timing can be assessed by varying the CS-US interval (Desmond & Moore, 1982).

Researchers do not agree on whether any brain region identified as crucial for the performance of robust CRs, such as the cerebellum, is actually involved in the learning process or, indeed, whether learning also depends on the integrity of other structures (Desmond & Moore, 1986). One possibility is that "learning the connection between a CS and the US" occurs within Purkinje cells (PCs) of cerebellar cortex, specifically at parallel fiber synapses. Contending views are that the critical connections are formed within the deep cerebellar nuclei or brain stem. It is well to get these issues in front of us before introducing implementation schemes. Thus armed, the reader can better judge their strengths and weaknesses. Some unresolved issues regarding the lesion data are reviewed here.

- Do the neural commands (motor programs) that result in a CR originate in the cerebellum? That is, can it be said that the cerebellum is a proximal *cause* of CR topography? We have recently performed a linear systems analysis of the relationship between the firing rate of single neurons in NIA and the position of the NM during conditioning trials (Berthier, Barto, & Moore, 1988). Regarding

a causative link, we find that in some NIA cells the relationship between rate of firing and position of the NM can be modeled by a nonrecursive (causal) digital filter (Hamming, 1983). Using a related approach, we estimate the transfer function between neural activity and NM position, and from this it is possible to write a differential equation relating the two variables. Some NIA cells with CR-predictive firing yield equations for second-order systems. These equations relate a cell's firing rate to the acceleration, position, and velocity of NM movement. It is worth noting that NM movement is linearly related to eyeball retraction. In fact, the sweep of the NM over the eye is caused by retraction of the globe. The mechanics of eyeball retraction are those of a Voight element consisting of elastic and viscous components, a classic textbook example of a second-order linear system. Hence, it is perhaps not surprizing that equations relating the firing of some NIA cells to the conditioned NMR are those of second-order linear systems.

- Do lesions of cerebellar cortex produce a complete and permanent loss of a previously acquired CR? This question is important in itself, but especially so because of the well-known theories of Marr (1969) and Albus (1971), who independently suggested that motor learning, including classical conditioning, involves cerebellar cortex in a fundamental way. Yeo and his colleagues were the first to show that HVI lesions disrupt CRs, typically by either eliminating them altogether or greatly reducing their amplitude (Yeo, Hardiman, & Glickstein, 1984). These studies have been extended to show that lesions of HVI must be complete in order to eliminate small amplitude responses that would normally be counted as CRs and to prevent recovery after extended post-operative training (Yeo & Hardiman, 1988). Lavond, Steinmetz, Yokaitis, and Thompson (1987) report small amplitude CRs and recovery following extended training in cases where HVI removed appears to have been complete, and so the issue remains in question.

- Do lesions of the inferior olivary nuclei cause a progressive decline of the CR resembling extinction as some investigators claim (McCormick, Steinmetz, & Thompson, 1985), or is it the case that such lesions merely disrupt normal cerebellar functioning and in this way bring about an immediate detrimental effect on performance (Yeo, Hardiman, & Glickstein, 1986)? This issue is as yet unresolved because experiments have yielded conflicting results. If lesions of the inferior olivary nuclei, particularly DAO, do result in experimental extinction, then this would support models built on the idea that climbing fibers from DAO to cerebellum carry the reinforcement signal from the US to sites of learning.

- Does stimulation of the DAO provide a reinforcing signal for learning in cerebellar cortex (Steinmetz et al., 1989)? Or is any learning in the cerebellum confined to NIA, which receives climbing fiber collaterals from DAO? Related to this question is the possibility that stimulation of DAO does not reinforce learning in the cerebellum at all. It may merely stimulate brain stem elements of the reflex pathway underlying the UR where learning might occur (Bloedel, 1987; Yeo, 1989).

There are other issues to be resolved among workers in the extended laboratory of the conditioned NMR. I have mentioned only those that bear on evaluating the implementation schemes suggested for each of the models outlined in subsequent sections. Each model has its own implementation scheme. They both assume that learning occurs through Hebbian mechanisms that involve synaptic modification through convergence of CS and US information onto single neurons (Byrne, 1987). They both assume that these synaptic modifications occur in cerebellar cortex (HVI) and that CRs are initiated by the action of PCs on NIA cells to which they project. The implementation for the SBD model assumes that learning occurs in cerebellar cortex, but one synapse before the PC or output stage (Moore & Blazis, 1989a, 1989b, 1989c). The other model, designated VET, is more complex and assumes that learning occurs within the brain stem as well as in cerebellar cortex. The cortical component assumes that learning occurs through modification and parallel fiber/PC synapses. In addition, it assumes that learning also occurs at the synapses of parallel fibers and Golgi cells (Moore, Desmond, & Berthier, 1989).

THE SBD MODEL

The SBD model has been described in detail elsewhere (e.g., Moore et al., 1986; Moore & Blazis, 1989a, 1989b, 1989c), and so a brief summary will suffice. The model is based on a single neuron-like processing unit that receives input from many potential CSs and a US. The processing unit adjusts the weights (synaptic efficacies) of the CS input so that future output of the unit matches its current output.

Equation 1 specifies that the output of this system, denoted $s(t)$, equals the weighted sum of its input from potential CSs and the US. The variable $s(t)$ is a linear function of its weighted input only within an allowed range imposed by the fact that the NM can only move so far (about 10 mm) as the eyeball retracts. A CS's contribution to the output of the element is computed as the product of the current strength of its representation, denoted $x(t)$ in the model, and a corresponding "synaptic" weight denoted $V(t)$. Formally, the output of the system at time t, denoted $s(t)$, equals the weighted sum of input from all CSs, where $x_i(t)$ refers to the magnitude of CS$_i$, $i = 1, \ldots, n$, at time t:

$$s(t) = \sum_{i=1}^{n} V_i(t)\, x_i(t) + \lambda'(t). \tag{1}$$

$\lambda'(t)$ is the US's contribution to $s(t)$.

In Equation 1, $x_i(t)$ represents the activation level of the ith member of a set

of potential CSs at discrete times t after onset (t represents successive time steps of 10-msec duration). The following specifications for x_i were dictated by two contraints: (a) generation of realistic response topography for a forward-delay paradigm with a favorable CS-US interval, and (b) generation of realistic interstimulus interval (ISI) functions. The optimal CS-US interval for NMR conditioning is generally taken to be 250 msec (Gormezano, 1972). When the CS_i begins, $x_i = 0.0$. It remains at 0.0 until $t = 7$, i.e., 70 msec after CS_i onset. At this point, x_i begins to increase in an S-shaped fashion. It levels off to a maximum value of 1.0 by $t = 30$ (300 mec after CS_i onset) and remains at this value until CS_i offset, at which time x_i begins to fall exponentially back to 0.0. Thus, according to Equation 1 the output of the model, $s(t)$, to CS_i conforms to the temporal map or *template* provided by x_i. As the number of training trials increases, the variable $V_i(t)$ increases, and the CR becomes increasingly robust. This process is reversed over a series of extinction trials.

Learning in the SBD model follows a modified Hebbian rule that states that changes of the synaptic weight of CS_i, ΔV_i, are proportional to the *difference* between the current output, $s(t)$, and the trace of preceding outputs, $\bar{s}(t)$. At time t, ΔV_i is computed as follows:

$$\Delta V_i(t) = c[s(t) - \bar{s}(t)]\,\bar{x}_i(t), \tag{2}$$

where c is a learning rate parameter, $0 < c \leq 1$.

The factor $\bar{x}_i(t)$ in Equation 2 specifies the degree to which the "synaptic junction" corresponding to CS_i is *eligible* for modification (Sutton & Barto, 1981). $\bar{x}_i$ is driven by the variable $x(t)_i$: After CS_i onset, it increases with the x_i, but with a lag of 30 msec. It remains at full strength as long as the CS_i is on and begins to decay to a baseline value of zero 30 msec after Cs_i offset. The rate of this decay is inversely related to CS_i duration whenever CS_i exceeds 250 msec.

Equation 2 does not contain an explicit term for the reinforcing action of the US. The US is important only insofar as it affects the term $s(t) - \bar{s}(t)$. The interaction of the two time-dependent variables associated with CS_i, $x_i(t)$ and $\bar{x}_i$, together with $s(t) - \bar{s}(t)$, govern the rate of learning and shape of ISI functions. Trial-wise learning curves reflect accumulated net changes in V_i occurring *within* each trial. Such changes occur before and after the occurrence of the US. For example, given the 10 msec time step used in our simulations (e.g., Moore et al., 1986), a trial with an ISI of 350 msec might involve over 400 computations of ΔV_i.

The term $\bar{s}(t)$ in Equation 2 can be thought of as a short-term decaying trace of the system's output from previous time steps. Alternatively, it can be interpreted as a prediction or expectation of output based on previous output. It is computed as follows:

$$\bar{s}(t+1) = \beta\bar{s}(t) + (1-\beta)s(t), \tag{3}$$

where $0 \leq \beta < 1$.

Simulation studies indicate that, with a 10 msec time step, optimal performance of the model requires that β be on the order of 0.6–0.7 (Blazis & Moore, 1987). With β in this range, Equation 3 approximates the inhibitory action of cerebellar Golgi cells on information flow through the granular layer of cerebellar cortex (Eccles, Sasaki, & Strata, 1967). This coincidence was exploited in implementing the model (Moore & Blazis, 1989a, 1989b, 1989c).

The foregoing assumptions enable the SBD model to simultaneously generate response topographies and ISI functions for both trace and forward-delay conditioning paradigms (Moore et al., 1986). In addition, it retains the original Sutton-Barto model's ability to describe multiple-CS phenomena such as blocking, higher-order conditioning, and conditioned inhibition (Barto & Sutton, 1982; Sutton & Barto, 1981). In agreement with experimental literature (Miller & Spear, 1985), the model does not predict extinction of conditioned inhibition.

Implementing the SBD model

Moore and Blazis's (1989a, 1989b) implementation of the SBD model is summarized in this section. We required that the implementation scheme meet the following criteria: (a) It had to involve the cerebellum and be consistent with its anatomy and physiology. (b) It had to account for the lesion data, namely the fact that lesions of cerebellar cortex (HVI) or associated brain stem circuits virtually eliminate the CR. (c) It had the propose neuronal loci where the learning rule (Equation 2) might be implemented. This meant proposing sites where CS information, the variable $\bar{x}$, converges with the reinforcement signal, $s - \bar{s}$. (d) It had to propose schemes for computing $\bar{s}$ via Equation 3 and $s - \bar{s}$. The last item held the key. Once overcome, the rest of the implementation fell into place.

Turning now to the details of the implementation, the output variable s, which expresses the form of the CR and is used in the learning rule, is generated by the action HVI PCs on neurons in NIA to which they project. Evidence supporting this construction was reviewed earlier. Next, s is transmitted with high fidelity through each of the synaptic links leading to AAN motoneurons and generation of the peripherially observed CR. One synapse before this stage, within SpoV, an efference copy of s peels off and ascends back to HVI via mossy fibers. This efference copy of s consists of two streams. One stream passes through the granular layer without modulation by Golgi cells. This stream gives rise to parallel fibers (axons of granule cells) that carry s information to other circuit components, including Golgi cells that modulate the other s stream. This modulation computes $\bar{s}$ (see Moore & Blazis, 1989a, 1989b, 1989c) and gives rise to parallel fibers carrying $\bar{s}$ information.

The existence of separate parallel fibers that carry s and $\bar{s}$ information, respectively, allow for computation of the reinforcement factor in Equation 2, $s - \bar{s}$, by Golgi cells. These Golgi cells are distinct from those that compute $\bar{s}$. The computation of $s - \bar{s}$ occurs as follows: Golgi cells receive two simultaneous

inputs from parallel fibers: an excitatory (depolarizing) input from the $\bar{s}$-carrying parallel fibers mentioned above and an inhibitory (hyperpolarizing) input from axon collaterals of PCs activated by s-carrying parallel fibers mentioned above. Notice that the algebraic sum of these inputs is $\bar{s} - s$, but because Golgi cells are inhibitory neurons, the effect of their axonal output on granule cells is proportional to $s - \bar{s}$, as required by the model.

In the implementation scheme, this output is directed to granule cells, different from those mentioned previously, which are activated by CSs via mossy fibers. CS information has been preprocessed such that the input to these granule cells from mossy fibers is proportional to the variable x.[3] The eligibility factor used in the learning rule, $\bar{x}$, presumably resides within x-activated granule cells (Sutton & Barto, 1981). Thus, these granule cells receive convergent input from mossy fibers carrying x-information and Golgi cell input carrying $s - \bar{s}$-information. This convergence allows for implementation of the learning rule for updating V by modified Hebbian mechanisms assumed by the model. The output of these granule cells is proportional to Vx, which in the one-CS case is equal to s.

Parallel fibers arising from these granule cells convey Vx to basket cells and PCs. The basket cells, which are inhibitory neurons, send axons to PCs on an adjacent, previously unmentioned group of parallel fibers. As Vx increases after CS onset, the accompanying increase in activation of basket cells causes the firing of PCs on the adjacent group of parallel fibers to decreases below their baserate of firing. This decrease causes *disinhibition of neurons in NIA, to which they* project. This, in turn, causes NIA cells to increase their firing rate and send an excitatory pulse of activation proportional to s through the efferent pathway for expression of the CR described previously. The penultimate link in this sequence are neurons in SpoV that return the current value of s to HVI for the next computation of ΔV.

Implications of the SBD Model

The complexity of the implementation scheme stems from considerations of anatomy and physiology. These considerations are elaborated elsewhere (Blazis & Moore, 1987; Moore & Blazis, 1989a, 1989b, 1989c). The most compelling evidence for the scheme comes from Berthier and Moore's (1986) study of how PCs in HVI respond during NMR conditioning.

Berthier and Moore (1986) recorded from single PCs in HVI during the asymptotic stages of two tone differential conditioning. PCs with CR-related firing patterns could be classified as either increasing or decreasing their baserate of firing whenever a CR occurred. Three cells increased firing for every one that decreased firing. Firing patterns of PCs could also be classified as either preceding or occurring simultaneously with CRs. All of the PCs that decreased their firing

[3] For discussion of this point, see Moore and Blazis (1989c).

did so before the CR occurred, as would be necessary if their activity were responsible for initiating CRs. PCs that increased their firing before the occurrence of CRs are implied by parallel fibers carrying Vx information. PCs that increase their firing simultaneously with CRs are implied by the two streams of s-carrying efference from SpoV used in the computation of $\bar{s} - s$. It remains to be determined whether we can objectively discriminate increases in PC firing that mirrors s from that mirroring $\bar{s}$. This caveat aside, the frequency distribution of firing patterns observed by Berthier and Moore (1986) are accounted for by the implementation scheme.

Behavioral Predictions

The SBD model predicts that the rate of CR acquisition in a trace conditioning paradigm (but not a forward-delay paradigm) is an increasing function CS duration, provided the interval between CS offset and US onset (trace interval) is sufficiently long, e.g., 300 milliseconds or more. The prediction follows directly from the model's assumption that the eligibility factor in the learning rule, $\bar{x}$, decays at a rate that is inversely related to the duration of the CS. The prediction is counterintuitive because it states that acquisition can be faster with a longer-than-optimal ISI than one nearer to optimal. Preliminary studies with an acoustic CS (Blazis & Moore, 1989) have born out this prediction, but only when the CS is sufficiently intense (e.g., 80 dB). The prediction is not supported with a CS on the order of 60 dB. In this case, acquisition rate appears to be dominated by ISI instead of CS duration, as in forward-delay conditioning.

I mention this particular experiment in order to point out that the SBD model does not yet provide a complete account of NMR conditioning. In this case, the model is incomplete because it says nothing about how CS intensity affects the variables x or $\bar{x}$. Part of the motivation for the experiment discussed earlier was to obtain information on how to incorporate these effects into the model. The SBD model also fails to take account of processes that might occur within intertrial intervals, for example, the "consolidation" effects from studies showing that rate of conditioning is a direct function of intertrial interval (Moore & Gormezano, 1977).

Physiological Predictions

The most important prediction from the implementation scheme is that learning occurs within the granular layer of cerebellar cortex. Testing this prediction will require experiments on cerebellar slices using designs similar to those employed by Coulter and Disterhoft to investigate long-term effects of NMR conditioning on hippocampal pyramidal cells (e.g., Coulter et al., 1989). It also remains to be proven that SpoV cells that fire in relation to CRs actually send *collateral efference copy mirroring CR waveform to HVI. All we can say with confidence* at this point is that cells in SpoV exist that show CR-related firing of the kind

needed to provide HVI with a current copy of the variable s (Ricciardi, Richards, & Moore, 1989). We also know that some SpoV cells send mossy fibers to HVI. We do not know that the two categories actually overlap.

The implementation scheme does not assign a role in learning to climbing fiber inputs from DAO. Additional studies are needed to determine whether this is justified. One reason for discounting the possible contribution of climbings fibers is that their low firing rate makes them poor candidates for providing efference copy about s for implementation of the learning rule. In addition, very few PCs observed by Berthier and Moore (1986) responded with a complex spike, indicative of climbing fiber input, when the US occurred. Nevertheless, the possibility that climbing fibers are important for learning cannot be ruled out without further experimental work (Ito, 1989; Moore & Berthier, 1987). In fact, Moore et al.'s (1989) implementation of the VET model, reviewed in the next section, assumes that learning in the cerebellum is reinforced by climbing fiber input elicited by the US.

THE VET MODEL

The SBD model is able to simulate response topography because it assumes that every potential CS provides the system with a fixed pattern of activation that serves as a template for the CR. We have speculated about how templates might be formed and the possible contributions of other brain regions, especially the hippocampus, to this process (Blazis & Moore, 1987). The SBD model basically sidesteps this issue. In addition, it is incapable of adaptively changing CR topography so as to simulate a number of paradigms. The SBD model cannot yield appropriate CR waveforms for the following cases:

- Trace conditioning. CR waveforms should peak just before the occurrence of the US, as in forward-delay paradigms, but the dynamics of the variable x do not permit this to happen. Instead, CR waveforms begin to fall toward baseline when CS offset occurs.
- Forward-delay conditioning with long CS-US intervals. The SBD model cannot simulate inhibition of delay. Since CR-waveform mirrors the template provided by the variable x, its latency and form are not influenced by the CS-US interval.
- Multiple CS-US intervals. Training with multiple CS-US intervals yields complex CR-waveforms. For example, a study by Millenson, Kehoe, and Gormezano (1977) showed that training with randomly mixed trials having CS-US intervals of 200 and 700 milliseconds gives rise to CRs with two peaks, each centered at a time of US onset.

The VET model overcomes these deficiencies. It is able to simulate appropriate CR waveforms for these cases because of features absent in the SBD model. These features include the following:

- CSs are provided with a temporal dimension through tapped delay lines that encode, not only the source of the stimulus, but also the time since the stimulus began. Another set of tapped delay lines encodes the time since the stimulus ceased. Hence, the model has timed-tagged input elements for both stimulus onset and offset (Equation 4).
- There are two neuron-like processing units that receive convergent input from CSs and the US. One unit (designated V) is the output device (Equation 5). It has modifiable synaptic weights that are changed according to an LMS rule resembling the Rescorla-Wagner model (Equation 6). The main difference from the Rescorla-Wagner model is that weight changes depend on local eligibility factors (Equation 7), a global ISI parameter (Equation 8), and on an additional reinforcement signal reflecting the expected time of occurrence of the US (Equation 9).
- This additional reinforcement signal is computed by the other processing unit, designated the E unit, which learns when the US occurs. Like the V unit, the E unit receives convergent input from CSs and the US, and it has modifiable synaptic weights that are changed according to a simple linear difference equation (Equation 11) that includes local eligibility factors (Equation 10) and the global ISI parameter defined in Equation 8.

A more formal treatment follows:

Architectural assumptions for the network have been described in detail elsewhere (Desmond & Moore, 1988; Moore et al., 1989). Basically, the onset and offset of each CS begins activation of separate tapped delay lines. The elements in the delay line are referred to as x_{ijk} elements because each element can be referenced by (a) its CS (i), (b) whether it is activated by the onset ($j = 1$) or offset ($j = 0$) of the CS, and (c) its number within the delay line (k). For example, element x_{208} belongs to the offset delay line for CS2, and is the eighth element activated in the delay line. The output of an x_{ijk} element (which is either 1 or 0) at time t is designated $x_{ijk}(t)$.

The x_{ijk} tapped delay line elements are activated sequentially, with a new element recruited every time step (10 ms). When activated, an x_{ijk} element changes value from 0 to 1, and remains at 1 for 10 time steps. Thus, for each trial beginning at time $t = 1$:

$$x_{ijk}(t) = \begin{cases} 1 & \text{if } \tau_{ij} + k - 1 \le t < \tau_{ij} + k + 9; \\ 0 & \text{otherwise} \end{cases} \quad (4)$$

where τ_{ij} is the onset time ($j = 1$) or offset time ($j = 0$) of CS i ($x_{ijk} = 0$ is CS i is not presented).

In addition to the x_{ijk} elements, the network has two higher order processors designated the V unit and E unit. Each x_{ijk} element gives off two taps, one of which projects to the V unit and the other to the E unit. The latter connections are modifiable, and the weights for these connections are referred to as V_{ijk} and E_{ijk}. All other connections are non-modifiable; these include: US connections with the V and E units, an E-unit projection to the V unit, and connections between adjacent x_{ijk} elements in the delay line.

The output of the network, $s(t)$, is derived from the US input and from the weighted sum of the V unit inputs, and is defined as:

$$s(t) = \sum_{i}\sum_{j}\sum_{k} V_{ijk}(t)x_{ijk}(t) + L(t) \tag{5}$$

where $s(t)$ is confined to the closed unit interval.

Changes in the V_{ijk} weights are given by the following expression:

$$\Delta V_{ijk}(t) = c\{L(t) - \hat{s}(t)\}h_{ijk}(t)\bar{x}_{ij}(t)r(t). \tag{6}$$

where:

c is a rate parameter, $0 < c \leq 1$.

$L(t)$ is the reinforcement, $0 \leq L(t) \leq \lambda$, where λ is analogous to the strength of the reinforcement during conditioning, $0 < \lambda \leq 1$. $L(t) = 0$ until the US occurs, at which time $L(t) = \lambda$.

$\hat{s}(t) = \sum\sum\sum V_{ijk}(t)x_{ijk}(t)$, and is confined to the closed unit interval.

$h_{ijk}(t)$ constitutes an eligibility trace for each V_{ijk} synapse, $0 \leq h_{ijk}(t) \leq 1$. This term has maximum value at the onset time of the element and decays geometrically. It is computed as follows:

$$h_{ijk}(t) = \begin{cases} 1.0 & \text{if } t = \tau_{ij} + k - 1; \\ (0.8)h_{ijk}(t-1) & \text{if } t > \tau_{ij} + k - 1; \\ 0.0 & \text{otherwise,} \end{cases} \tag{7}$$

$\bar{x}_{ij}(t)$ is an *overall CS eligibility* for onset and offset processes, $0 \leq \bar{x}_{ij}(t) \leq 1$. This function governs the rate of conditioning that occurs at a given interstimulus interval. $\bar{x}_{ij}(t)$ is globally available to all V_{ijk} and E_{ijk} synapses. The equations described below approximate the empirically observed inverted-U-shaped function found in rabbit nictitating membrane conditioning:

$$\bar{x}_{ij}(t) = \begin{cases} (.05)(t - \tau_{ij}) - 0.25 & \text{if } \tau_{ij} + 6 < t < \tau_{ij} + 25; \\ (-1/475)(t - \tau_{ij}) + (500/475) & \text{if } \tau_{ij} + 25 \leq t < \tau_{ij} + 500; \\ 0.0 & \text{otherwise.} \end{cases} \tag{8}$$

$r(t)$ is the output of the E unit, and represents the temporal expectation of reinforcement, $0 \leq r(t) \leq \lambda$. It is defined as follows:

$$r(t) = \max\{E_{ijk}(t)\Delta x_{ijk}(t) \mid i = 1, \ldots, n; j = 0, 1; k = 1, \ldots, N\} \tag{9}$$

where:

$$\Delta x_{ijk}(t) = \begin{cases} 1 & \text{if } x_{ijk}(t) - x_{ijk}(t-1) = 1; \\ 0 & \text{otherwise,} \end{cases} \tag{10}$$

and E_{ijk} are the connection weights of the input elements onto the E unit. Changes in these weights are given by:

$$\Delta E_{ijk}(t) = c[L(t) - r(t)]\Delta x_{ijk}(t)\bar{x}_{ij}(t) \tag{11}$$

Implementing the VET Model

The implementation criteria for the VET model were the same as for the SBD model. The two schemes share many common features, e.g., they both assume that CRs are generated by the disinhibiting action of HVI PCs on NIA neurons, and Golgi cells play a crucial role in both. The scheme assumes that the time-tagged input elements associated with a CS ascend to cerebellar cortex via mossy fibers. They synapse within the granule layer, and with no modulation are assigned to a corresponding set of parallel fibers. The parallel fibers that carry CS information synapse on both PCs and Golgi cells. Notice that the implementation assumes that the tapped delay line architecture exists outside the cerebellum, possibly within the brain stem reticular formation (Scheibel & Scheibel, 1967). The anatomical justification for this assumption is discussed elsewhere (Desmond & Moore, 1988; Moore et al., 1989).

These synapses are modifiable. Synapses on PCs are sites where Equation 6 is implemented, and hence these cells are the V units. Synapses on Golgi cells are sites where Equation 11 is implemented, and hence these cells are the E units. Both sets of modifiable synapses are changed when the US occurs to the extent that they are eligible. The US triggers a climbing fiber volley that causes these synapses to undergo synaptic depression via mechanisms of long term depression (LTD) identified by Ito (1989) and others (e.g., Crepel & Krupa, 1988). With learning, CS input causes V and E units to decrease their baserate of firing. For V units, this decrease initates a CR. For E units, this decrease disinhibits certain granule cells. These granule cells receive input from brain stem neurons, possibly in SpoV, which also undergo learning due to the convergence of CS and US information. Although no learning rule is specified, the SBD (or SB) model suffices provided the variable x in Equation 1 increases rapidly to a plateau at CS onset and decays slowly at CS offset.

With learning, the output (rate of firing) of these brain stem units consists of a short latency plateau that extends well beyond the offset of the CS. This output provides a uniform and long lasting stream of excitatory input to granule cells. The E units, however, gate this excitation and prevent it from exciting parallel fibers that synapse on the V units. As learning builds up in the E units, this gate

is opened, but only during times near the expected occurrence of the US. Thus, E units provide the second reinforcing event necessary for modification of CS-input synapses on the V units so that they express appropriately timed CR waveforms.

Implications of the VET Model

The VET model simulates virtually all of the behavioral phenomena encompassed with the SBD model, but unlike that model, it has the added feature of predicting realistic S-shaped acquisition curves. Unlike the SBD model, however, it cannot simulate second-order conditioning. As in the Rescorla-Wagner model, connection weights are strengthened only in the presence of the US. Desmond and Moore (1988) describe several novel predictions of the VET model. One prediction is that lengthening the duration of a CS after trace conditioning should result in double peaked CR waveforms, reflecting contributions of both onset and offset tapped delay elements. The weights of offset elements are normally masked by those of the onset elements, but lengthening the CS exposes these offset elements, and CRs with two peaks emerge.

The physiological implications of the implementation scheme are many. The most interesting implication is the possibility that cerebellar Golgi cells express LTD at parallel fiber synapses in a manner analogous to that of PCs. There appears to be no evidence on this point in the literature. Another implication of the scheme is that climbing fibers from DAO do, in fact, reinforce learning. In order for this possibility to be taken seriously, it would be necessary to record from PCs (and Golgi cells) in HVI during the initial stages of CR acquisition. This was not done in the Berthier and Moore (1986) study, nor in any other study, for methodological reasons: It is virtually impossible to record from single neurons in an awake animal for the hundreds of trials normally required to obtain robust CRs. Nevertheless, there are ways around this problem we are pursuing in our laboratory. Finally, the scheme implies the existence of neurons in the brain stem that project to HVI and fire in accordance with the scheme's requirements. We have seen a number of candidate neurons in recordings from cells in NIA, RN, SpoV. Cells in RN and SpoV project to HVI, and it is possible, though not proven in rabbit, that NIA cells send mossy fibers to HVI as axon collaterals.

CONCLUDING REMARKS

The two models and implementation schemes are quite different, but not mutually exclusive. The VET model implies a neural network architecture well suited for forming appropriate CR waveforms for a wide range of circumstances. The output of this network need not be regarded as input to motoneurons. Instead, it could be regarded as a template used by another learning system responsible for such

things as generating CRs and implementing second-order conditioning. Such a system might resemble the SBD model or some other supervised learning (error correction) algorithm.

Such a hybrid model would not encompass phenomena that both models fail to address: intertrial interval effects, CS intensity, stimulus generalization and discrimination. These phenomena require a richer representation of CS input to learning networks than have been considered by either model to date. Desmond (1988) has developed one approach that can potentially address these topics. It represents CSs as planar arrays of elements through which activation spreads and decays in an orderly, yet stochastic manner. The planar array approach follows directly from the foundations provided by the SBD and VET models, and we might anticipate as abundant a harvest of interesting implications as have sprung from its forerunners.

ACKNOWLEDGMENT

Preparation of this chapter and the author's research program were supported by grants from the Air Force Office of Scientific Research and the National Science Foundation.

REFERENCES

Albus, J.S. (1971). A theory of cerebellar function. *Mathematical Bioscience, 10,* 25–61.

Barto, A.G., & Sutton, R.S. (1982). Simulation of anticipatory responses in classical conditioning by a neuron-like adaptive element. *Behavioural Brain Research, 4,* 221–235.

Berthier, N.E., Barto, A.G., & Moore, J.W. (1988). Linear systems analysis of cerebellar deep nuclei cells during performance of the classically conditioned eyeblink. *Society for Neuroscience Abstracts, 14,* 1239.

Berthier, N.E., & Moore, J.W. (1986). Cerebellar Purkinje cell activity related to the classically conditioned nictitating membrane response. *Experimental Brain Research, 63,* 341–350.

Blazis, D.E.J., & Moore, J.W. (1987). *Simulation of a classically conditioned response components of the input trace and a cerebellar neural network implementation of the Sutton-Barto-Desmond model.* Computer and Information Science technical report 87-74, University of Massachusetts, Amherst, MA.

Blazis, D.E.J., & Moore, J.W. (1989). Conditioned stimulus duration: Behavioral assessment of a prediction of the Sutton-Barto-Desmond model. *Society for Neuroscience Abstracts, 15,* 506.

Bloedel, J.R. (1987). Technical comment. *Science, 238,* 1728–1729.

Byrne, J.H. (1987). Cellular analysis of associative learning. *Physiological Reviews, 67,* 329–439.

Churchland, P.S. (1986). *Neurophilosophy: Toward a unified science of the mind-brain.* Cambridge, MA: MIT Press.

Coulter, D.A., Lo Turco, J.J., Kubota, M., Disterhoft, J.F., Moore, J.W., & Alkon, D.L. (1989). Classical conditioning reduces amplitude and duration of calcium dependent afterhyperpolarization in rabbit hippocampal pyramidal cells. *Journal of Neurophysiology, 61,* 971–981.

Crepel, F., & Krupa, M. (1988). Activation of protein kinase C induces a long-term depression of

glutamate sensitivity of cerebellar Purkinje cells. An in vitro study. *Brain Research, 458,* 397–401.

Desmond, J.E. (1988). *Temporally adaptive conditioned responses: Representation of the stimulus trace in neural-network models.* Computer and Information Science technical report 88–80. University of Massachusetts, Amherst, MA.

Desmond, J.E., & Moore, J.W. (1982). A brain stem region essential for the classically conditioned but not unconditioned nictitating membrane response. *Physiology & Behavior, 28,* 1029–1033.

Desmond, J.E., & Moore, J.W. (1986). Dorsolateral pontine tegmentum and the classically conditioned nictitating membrane response: analysis of CR-related single-unit activity. *Experimental Brain Research, 65,* 59–74.

Desmond, J.E., & Moore, J.W. (1988). Adaptive timing in neural networks: The conditioned response. *Biological Cybernetics, 58,* 405–415.

Eccles, J.C., Sasaki, K., & Strata, P. (1967). A comparison of the inhibitory action of Golgi and basket cells. *Experimental Brain Research, 81–94.*

Gabriel, M. (1988). An extended laboratory for behavioral neuroscience: A review of *Classical conditioning* (third edition). *Psychobiology, 16,* 79–81.

Gormezano, I. (1972). Investigations of defense and reward conditioning in the rabbit. In A.H. Black & W.F. Prokasy (Eds.), *Classical conditioning II: Current research and theory* (pp. 151–181). New York: Appleton-Century-Crofts.

Gormezano, I., Prokasy, W.F., & Thompson, R.F. (Eds.) (1987). *Classical conditioning* (third edition). *Hillsdale, NJ:* Lawrence Erlbaum Associates.

Hamming, R.W. (1983). *Digital filters.* New York: Prentice-Hall.

Ito, M. (1989). Long-term depression. *Annual Review of Neuroscience, 12,* 85–102.

Lavond, D.G., Steinmetz, J.E., Yokaitis, M.H., & Thompson, R.F. (1987). Reacquisition of classical conditioning after removal of cerebellar cortex. *Experimental Brain Research, 67,* 569–593.

Marr, D. (1969). A theory of cerebellar cortex. *Journal of Physiology, 202,* 437–470.

McCormick, D.A., Steinmetz, J.E., & Thompson, R.F. (1985). Lesions of the inferior olivary complex cause extinction of the classically conditioned eyeblink response. *Brain Research, 359,* 120–130.

Millenson, J.R., Kehoe, E.J., & Gormezano, I. (1977). Classical conditioning of the rabbit's nictitating membrane response under fixed and mixed CS-US intervals. *Learning and Motivation, 8,* 351–366.

Miller, R.R., & Spear, N.E. (Eds.) (1985). *Information processing in animals: Conditioned inhibition.* Hillsdale, NJ: Lawrence Erlbaum Associates.

Moore, J.W. (1979). Brain processes and conditioning. In A. Dickinson & R.A. Boakes (Eds.), *Mechanisms of learning and motivation: A memorial volume to Jerzey Konorski* (pp. 111–142). Hillsdale, NJ: Lawrence Erlbaum Associates.

Moore, J.W., & Berthier, N.E. (1987). Purkinje cell activity and the conditioned nictitating membrane response. In M. Glickstein, C. Yeo, & J. Stein (Eds.), *Cerebellum and neuronal plasticity* (pp. 339–352). New York: Plenum.

Moore, J.W., & Blazis, D.E.J. (1989a). Cerebellar implementation of a computational model of classical conditioning. In P. Strata (Ed.), *The olivocerebellar system in motor control* (pp. 387–399). Berlin: Springer-Verlag.

Moore, J.W., & Blazis, D.E.J. (1989b). Simulation of a classically conditioned response: A cerebellar neural network implementation of the Sutton-Barto-Desmond model. In J.H. Byrne & W.O. Berry (Eds.), *Neural models of plasticity: Experimental and theoretical approaches* (pp. 187–207). San Diego: Academic Press.

Moore, J.W., & Blazis, D.E.J. (1989c). Conditioning and cerebellum. In M.A. Arbib & S. Amari (Eds.), *Dynamic interactions in neural networks: Models and data* (pp. 261–277). New York: Springer-Verlag.

Moore, J.W., Desmond, J.E., & Berthier, N.E. (1989). Adaptively timed conditioned responses and the cerebellum: A neural network approach. *Biological Cybernetics, 62,* 17–28.

Moore, J.W., Desmond, J.E., Berthier, N.E., Blazis, D.E.J., Sutton, R.S., & Barto, A.G. (1986). Simulation of the classically conditioned nictitating membrane response by a neuron-like adaptive element: Response topography, neuronal firing, and interstimulus intervals. *Behavioural Brain Research, 21,* 143–154.

Moore, J.W., & Gormezano, I. (1977). Classical conditioning. In M.H. Marx & M.E. Bunch (Eds.), *Fundamentals and applications of learning* (pp. 87–120). New York: Macmillan.

Ricciardi, T.N., Richards, W.G., & Moore, J.W. (1989). Single unit activity in spinal trigeminal oralis and adjacent treticular formation during classical conditioning of the rabbit nictitating membrane response. *Society for Neuroscience Abstracts, 15,* 507.

Robinson, D.A. (1981). The use of control systems analysis in the neurophysiology of movement. *Annual Review of Neuroscience, 4,* 463–503.

Robinson, D.A. (1989). Integrating with neurons. *Annual Review of Neuroscience, 12,* 33–45.

Scheibel, M.E., & Scheibel, A.B. (1967). Anatomical basis of attention mechanisms in vertebrate brains. In G.C. Quarton, T. Melnechuk, & F.O. Schmitt (Eds.), *The neurosciences. A study program* (pp. 577–602). New York: Rockefeller University Press.

Steinmetz, J.E., Lavond, D.G., & Thompson, R.F. (1989). Classical conditioning in rabbits using pontine nucleus stimulation as a conditioned stimulus and inferior olive stimulation as an unconditioned stimulus. *Synapse, 3,* 225–233.

Sutton, R.S., & Barto, A.G. (1981). Toward a modern theory of adaptive networks. Expectation and prediction. *Psychological Review, 88,* 135–170.

Yeo, C.H. (1989). The inferior olive and classical conditioning. In P. Strata (Ed.), *The olivocerebellar system in motor control* (pp. 363–373). Berlin: Springer-Verlag.

Yeo, C.H., & Hardiman, M.J. (1988). Loss of conditioned responses following cerebellar cortical lesions is not a performance deficit. *Society for Neuroscience Abstracts, 14,* 3.

Yeo, C.H., Hardiman, M.J., & Glickstein, M. (1984). Discrete lesions of the cerebellar cortex abolish the classically conditioned nictitating membrane response of the rabbit. *Behavioral Brain Research, 13,* 261–266.

Yeo, C. H., Hardiman, M. J., & Glickstein, M. (1986). Classical conditioning of the nictitating membrane response of the rabbit. IV. Lesions of the inferior olive. *Experimental Brain Research, 63,* 81–92.

Neuroscience Research, 10 (1991) 260–279

NEURES 00434

Single-unit activity in red nucleus during the classically conditioned rabbit nictitating membrane response

John E. Desmond * and John W. Moore

Department of Psychology, University of Massachusetts, Amherst, MS (U.S.A.)

(Received 9 October 1990; Revised version received 12 December 1990; Accepted 14 December 1990)

Key words: Red nucleus; Conditioned response; Classical conditioning; Learned movements; Eye blink

SUMMARY

Previous investigations have suggested that the cerebellum and associated brainstem structures, including the red nucleus, are essential for the expression of the classically conditioned nictitating membrane (NM) response. The present study examined the firing patterns of extracellularly-recorded single units in the red nucleus of the awake rabbit during differential conditioning. Tones were used as conditioned stimulus (CS+ and CS−) and periocular electrostimulation was used as the unconditioned stimulus (US). Most units exhibited one or more changes in firing rate during the presentation of the CS, and increases in firing were much more common than decreases. The onset of some of these changes appeared to be time-locked to the onset of the CS ('CS-locked' responses), while other changes were time-locked to the onset of the CR ('CR-locked' responses). About one-third of all CS-locked changes were CR-dependent, meaning that the neuronal response was reduced when the CR did not occur. About two-thirds of *all CR-locked responses preceded the onset of the CR*, and lead times varied considerably across units. Many CR-locked units were located in what has been described as a dorsal face region of the red nucleus. Most units responded to the US, and some of the US responses were CR-dependent: i.e., a smaller US response was evoked when a CR preceded the US than when the CR was absent. Our results support the notion that cerebellum–brainstem circuits are involved in generating NM CRs.

INTRODUCTION

Although it is widely accepted that rubrospinal neurons are involved in the control of movement, the precise role of these cells is not understood [40]. In some tasks, red nucleus cells begin to fire after movement is initiated [48,49], suggesting that the red nucleus participates in feedback control of movement or in movement termination. It has been demonstrated that activation of red nucleus neurons can inhibit somatosensory responses [9], and thus movement-related red nucleus activity may serve to filter out peripheral sensations during movements [53]. Other evidence suggests that peripheral feedback has little to do with the firing patterns of red nucleus cells. For example, red nucleus activity precedes movement by substantial amounts in some tasks [22,23,39], and it has been shown that movement-related patterns of red nucleus activity are not altered by

* *Present address:* J.E. Desmond, EEG Systems Laboratory, 51 Federal Street, Suite 401, San Francisco, CA 94107, U.S.A.

Correspondence: J.W. Moore, Department of Psychology, University of Massachusetts, Amherst, MA 01003, U.S.A.

an interruption of the movement[24]. Such results suggest that red nucleus activity is more related to motor commands than to peripheral feedback [33]. These motor commands may be encoding the velocity of the intended movement [6,24,34]. Other sets of experiments demonstrate that red nucleus firing can be time-locked to a conditioned stimulus (CS) or go-signal as well as the movement itself [1,39,57], suggesting that the red nucleus may generate phasic movement-triggering signals. The plasticity required for these CS-locked signals could be intrinsic to the red nucleus [47,60].

In recent years, investigations of the rabbit nictitating membrane (NM) response have revealed that specific regions of the cerebellum, as well as brainstem structures associated with the cerebellum, including the red nucleus, are necessary for the normal expression of the classically conditioned response (CR). Lesions of nucleus interpositus [7,36,62], cerebellar cortex [37,63], middle cerebellar peduncle [38], superior cerebellar peduncle [41], inferior olive [42,61,64], and red nucleus or rubrobulbar tract [54–56] produce disruption of the CR. Microinfusion of GABA antagonists into the red nucleus also disrupt the conditioned response [28]. Single-unit recording studies in cerebellar cortex [4,19] and deep cerebellar nuclei [5,43] have also revealed conditioning-related unit activity that precedes the onset of the CR.

The present study investigated whether similar conditioning-related unit activity could also be observed in the red nucleus. A large body of literature indicates that efferents from nucleus interpositus project contralaterally to the red nucleus. Many cells of the caudal red nucleus in turn send contralaterally-projecting rubrobulbar tract fibers to the brainstem and spinal cord. Consistent with these observations, conditioning deficits from unilateral cerebellar interpositus or cortex lesions involve the ipsilateral NM response, whereas unilateral red nucleus lesions produce deficits in the contralateral eye. Thus, we investigated the single-unit activity in the red nucleus by recording on the side contralateral to the conditioned eye. The purpose of this study was to characterize the firing patterns of red nucleus units to the CS, the unconditioned stimulus (US) and the CR. *

MATERIALS AND METHODS

A total of 24 New Zealand albino rabbits served as subjects in this study. The training and recording procedures were similar to those described by the authors for recording in the dorsolateral pontine tegmentum [10]. A differential conditioning procedure was used in order to obtain trials with and without CRs. The CSs used were tones of 1200 and 600 Hz and of 350-ms duration and 75-dB intensity (re. 20 $\mu N/m^2$). Each subject was randomly assigned as 1200 + /600 − (i.e. CS + was 1200 Hz, CS − was 600 Hz) or 600 + /1200 − . The intertrial interval was 20 s. White noise of 65-dB intensity was on continually. The US, an electrostimulation of 0.05–0.5 ms duration and 1-mA intensity delivered to the periocular region of the right eye, co-terminated with the CS + . Movement of the right NM was measured using a minitorque potentiometer that was connected to the NM by a suture [46]. For CS + trials, a CR was defined as a movement of the NM that begins after CS onset and before US onset. For CS − trials, which were not contaminated by a UR, a CR was defined as any movement of the NM that begins after CS onset. This movement appears as an upward deflection of the NM trace in Figures 3, 5, and 7 below. Trials in which a CR occurred are referred to as 'CR trials'; trials in which a CR was absent are referred to as 'no-CR trials' (see Fig. 3B).

* These data have been reported in abstract form[11].

The rabbits were trained for 2–3 days (100 trials/day, 50 to CS + and 50 to CS − presented in a pseudorandom sequence) and then surgically prepared for unit recordings. We intentionally began recordings before the rabbits learned to completely differentiate CS + and CS −, because an incomplete discrimination increases the probability that both CR and no-CR trial types occur for each CS. Obtaining both trial types was useful for assessing the CR-relatedness of the neuronal activity. For example, in Figure 3B, the spikes that occurred on CR trials (labelled 'CR spikes') exhibited a marked increase in firing shortly after the onset of the CS (the arrow labelled 'CS-locked' indicates the onset of the increase, and the meaning of this label is explained below). In contrast, the no-CR spikes (i.e., spikes which occurred on no-CR trials), exhibited only a slight increase in firing. The difference in firing on CR and no-CR trial types could not have been due to the CS alone, because the same CS (600 Hz) was present on both trial types. Thus, the difference in firing can be attributed to the presence or absence of the CR.

To surgically prepare a rabbit for unit recordings, the rabbit was anesthetized with a ketamine (40 mg/kg) – acepromazine (1 mg/kg) mixture (i.m.) [29]. A small hole for recording was drilled on the left side of the skull, and 3 additional holes were drilled for anchor screws. A recording chamber was cemented in place and the rabbit was allowed to recover for 2 days.

For unit recordings, the head of the rabbit was held motionless by fastening the recording chamber to a support bar. A tungsten microelectrode of 1–5 MΩ impedance was lowered through the recording hole into the brainstem during presentation of CS + and CS − trials. Unit activity and NM movement were taped for off-line analysis using a modified video cassette recorder (Vetter Co., model 420). Recording sites were marked at the end of the session by passing cathodal current (20 μA for 10 s) through the recording electrode. A maximum of 3 recording tracks were made for each rabbit. The rabbits were then sacrificed with sodium pentobarbital and transcardially perfused for subsequent histological identification of the recording tracks.

Data analysis

For data analysis, tape-recorded neuronal activity and NM responses were digitized using an Apple IIe microcomputer. Spikes were window-discriminated; the time of occurrence of each spike, relative to the trial onset, was recorded to the nearest 250 μs. The NM response was sampled at 200 Hz. The data were then transferred to a Sun 3 workstation for subsequent analysis.

Each trial was digitized for a total of 1.5 s. It is convenient to divide this time into 3 distinct periods: a 350-ms pre-CS period, a 350-ms CS period, and an 800-ms US period. This report describes changes in neuronal firing during the CS period and the US period. A change in firing is defined simply as a deviation from the baseline firing rate. Onset times, durations and magnitudes of these changes were measured using *cusums*, which are plots of cumulative spike counts over time from which baseline (i.e. pre-CS period) firing has been subtracted [16,23,24]. The slope of the cusum plot is the discharge rate above or below the baseline firing rate, and is referred to as the *depth of modulation* (DOM). To quantify changes in firing we inspected cusums that were averaged over trials. Onset time of a change was measured at the time when the slope of the averaged cusum deviated from zero. The duration was measured from the onset time to the time at which the cusum slope returned to zero. The magnitude of a change in firing was quantified by the DOM.

CS-period changes. Changes in firing during the CS period were classified as either *CS-locked* or *CR-locked*. CS-locked changes occurred at a constant latency relative to the

time of CS onset. In contrast, CR-locked changes occurred at a constant latency relative to the time of CR onset. Raster plots of unit activity and behavioral responses were used to assess whether a change was CS-locked or CR-locked. To accomplish this, NM responses were sorted by onset latency and displayed along with the corresponding unit activity, in the manner illustrated in Figures 3, 5, and 7. Both peri-stimulus and peri-response raster plots were constructed for each unit. In a peri-stimulus plot, such as the one depicted in Figure 3A, two long vertical lines are used to designate CS and US onsets (the US line also indicates the termination of the CS). Time to the left of the CS line is the pre-CS period, between the CS and US lines is the CS period, and to the right of the US line is the US period. For peri-response plots, such as the one depicted in Figure 3F, each trial is aligned on the CR onset time, which is depicted by a single vertical line. For both peri-stimulus and peri-response plots, the top traces represent NM responses ordered by onset latency, and the middle traces show the corresponding firing patterns for the unit. At the bottom of the plot is a histogram showing cumulative spike counts in 5-ms time bins.

CS-locked unit activity exhibited relatively constant response latencies on peri-stimulus plots and exhibited shifts in onset latency on peri-response plots, whereas the converse was true for CR-locked unit activity. For example, panels A, B, and C of Figure 5 depict CS + peri-stimulus plot, CS − peri-stimulus plot, and peri-response plot, respectively, for a unit that exhibited a CS-locked and a CR-locked change in firing. In panels A and B, the CS-locked change is seen to begin at a relatively constant latency after CS onset, whereas the onset of the CR-locked change in firing increases as the onset of the CR increases (the two changes are indicated with arrows in panel B). In the peri-response plot of panel C, which depicts CR trials that appear in both panels A and B, the CR-locked change in firing begins at a relatively constant latency prior to the onset of the CR, and the CS-locked change is seen to shift.

In this report, CS-locked changes are quantified in terms of onset latency, duration, and DOM. CR-locked changes are quantified only in terms of onset latency and DOM, because duration of CR-locked changes was often difficult to measure due to the overlapping occurrence of US-elicited responses. For both CS-locked and CR-locked cases, changes in firing did not appear to depend on whether CS + or CS − was presented. Rather, the most relevant variable to influence firing appeared to be whether or not the CS elicited a CR. In general, the units we recorded displayed the following characteristics:

(1) If a unit exhibited a CR-locked change, then this change occurred on CR trials and failed to occur on no-CR trials, regardless of whether the CS was CS + or CS − (e.g., see Fig. 5D and E).

(2) CS-locked changes in firing were classified as either CR-dependent or non-CR-dependent (discussed further in the Results section). If a unit exhibited a non-CR-dependent CS-locked change, then the change was observed on both CS + and CS − trials, and the characteristics of the firing were not altered by the presence or absence of a CR (e.g., Fig. 3C and D). However, if the CS-locked change was CR-dependent, then, regardless of whether CS + or CS − was presented, the DOM of the change was greater on CR trials than on no-CR trials (e.g., Fig. 3A and B).

Thus, CS + and CS − trials were pooled in computing onset latency, duration, and DOM of firing changes.

US-evoked responses. Inspection of cusums was satisfactory for measuring latencies of CS-locked or CR-locked changes. However, for precise measurement of short-latency

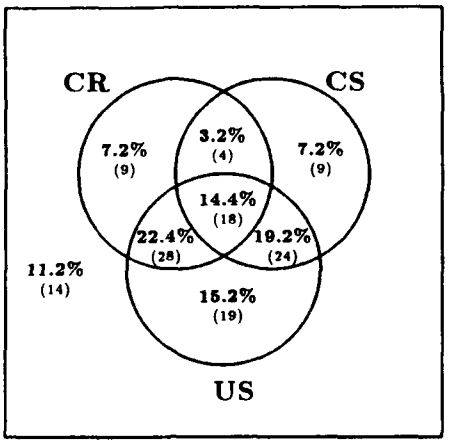

Fig. 1. Venn diagram illustrating the percentage of units (with raw numbers in parentheses) exhibiting CR-locked, CS-locked, or US-evoked responses. The CS-locked numbers include both CR-dependent and non-CR-dependent responses.

US-evoked responses it was necessary to display the taped neuronal activity on a storage oscilloscope (Tektronix model 5111A). * The latency of the US response was obtained by measuring the time between US onset and the onset of the first spike on several trials and computing a mean. For the few cells that responded to the US with an initial decrease in firing, the latency was measured at the time of the last spike before the rate decreased.

RESULTS

A total of 125 units was recorded from the red nucleus. These units were located in both magnocellular and parvocellular divisions of the nucleus according to the rabbit atlas of Gerhard [21]. ** Units were characterized by the types of changes in firing observed in the CS period and the US period. Figure 1 summarizes in Venn diagram form the percentages of units with CS-locked, CR-locked, or US-evoked changes, or any combination of these three. The raw number of units in each category appears in parentheses below the percentage. Thus, as an example, the figure indicates that 18 units (14.4%) exhibited both CS-locked and CR-locked changes *and* responded to the US. Chi-square analyses indicated that the three types of responses were independent: i.e., the presence of one type of response did not make it any more or less likely that one of the other types of responses would be present.

In the following sections, we describe the CS-period and US-period changes in firing that were observed in terms of onset latency, duration, and DOM. Because we are

* We use the term 'US-evoked' rather than 'US-locked' because some of the units exhibited more than one change in firing during the US period. Some of the longer latency changes in firing may have been a mixture of US-locked and UR-locked responses, and we did not attempt to separate these components.

** We did not attempt to classify an individual unit as magnocellular or parvocellular, as it is difficult to precisely delimit these regions in rabbit. Other investigators of cat [30] and rabbit [44] red nucleus have also noted the difficulties in delimiting magnocellular a and parvocellular regions, and Holstege and Tan [30] have suggested that the red nucleus should be subdivided based upon the projections of the cells as an alternative to the classical magnocellular and parvocellular divisions.

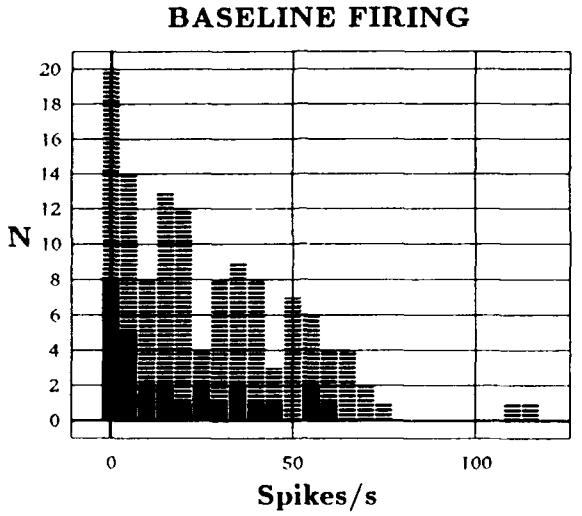

Fig. 2. Frequency distribution of baseline firing rates for all red nucleus units, measured from the pre-CS period. Solid bars represent units that (a) exhibited CR-locked firing that (b) preceded the behavior and (c) had $|DOM| \geq 25$ (these units are referred to as the 'select subpopulation.') Striped bars are units that are not in the select subpopulation. For example, at the 5 spikes/s midpoint, there are 14 units comprised of 5 select-subpopulation and 9 non-select-subpopulation units.

interested in cells that may have a direct causal role in the generation of the CR, we defined a *select subpopulation* of units that had the following characteristics: (a) the unit had a CR-locked change in firing, (b) the change consistently preceded the onset of the CR, and (c) the absolute value of the DOM of the change was greater than or equal to 25 spikes/s (i.e., $|DOM| \geq 25$). * A total of 28 units comprised the select subpopulation.

The frequency distribution of baseline firing rates for all units (rates measured from the pre-CS period) is illustrated in Figure 2. In this and subsequent figures, the height of a solid black bar represents the number of units from the select subpopulation. The height of a striped bar represents the total number of units, including the number in the select subpopulation. (As an example, the figure indicates that a total of 14 units had a baseline firing rate of approximately 5 spikes/s. Five of these units belonged to the select subpopulation.) The mean baseline firing rate was 26.8 spikes/s (median = 20.8, SD = 23.3). The figure shows that for both the general population and the select subpopulation, a considerable number of units had almost no baseline activity. These units were detected during the gradual descent of the electrode through the red nucleus by virtue of the units' responses to the CS, US, or CR. Units of the select subpopulation fired at a mean baseline rate of 18.3 spikes/s (median = 12.2, SD = 19.2). Units not in the select subpopulation fired at a faster rate of 29.2 spikes/s (median = 21.6, SD = 23.9). The difference in median rates is statistically significant (Mann-Whitney $U(28, 97) = 940$, $P < 0.05$, two-tailed).

* Absolute value is specified to include units that exhibited a decrease in firing rate. For such units, a DOM ≤ -25 spikes/s would put them in the select subpopulation. None of the relatively few units that showed CR-locked decreases in firing met this criterion. The value of 25 spikes/s was selected because of the ease in which a DOM of this magnitude or greater could be recognized by visual inspection of raster plots.

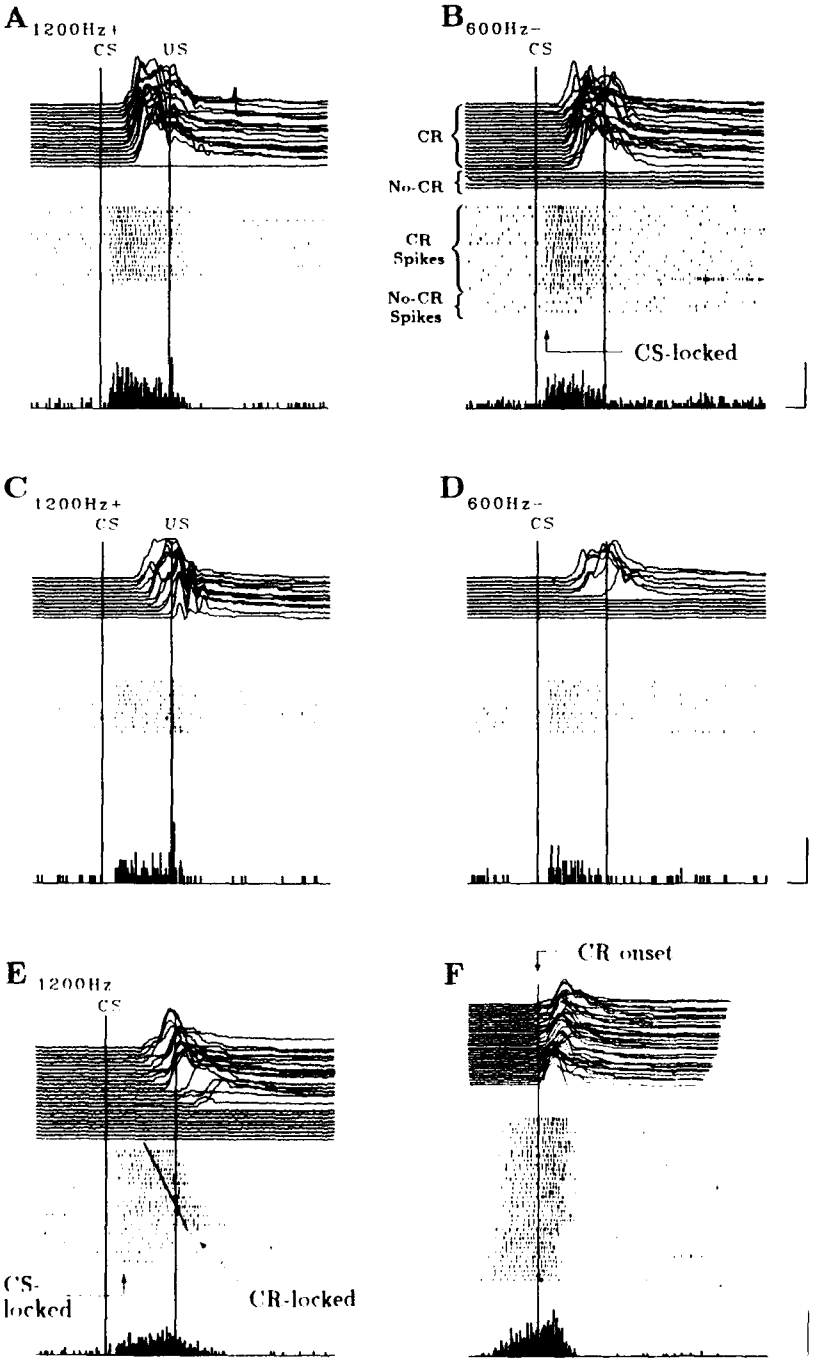
A
1200Hz+
CS
US
B
600Hz−
CS
CR
No-CR
CR Spikes
No-CR Spikes
CS-locked
C
1200Hz+
CS
US
D
600Hz−
CS
E
1200Hz
CS
CS-locked
CR-locked
F
CR onset

Fig. 3.

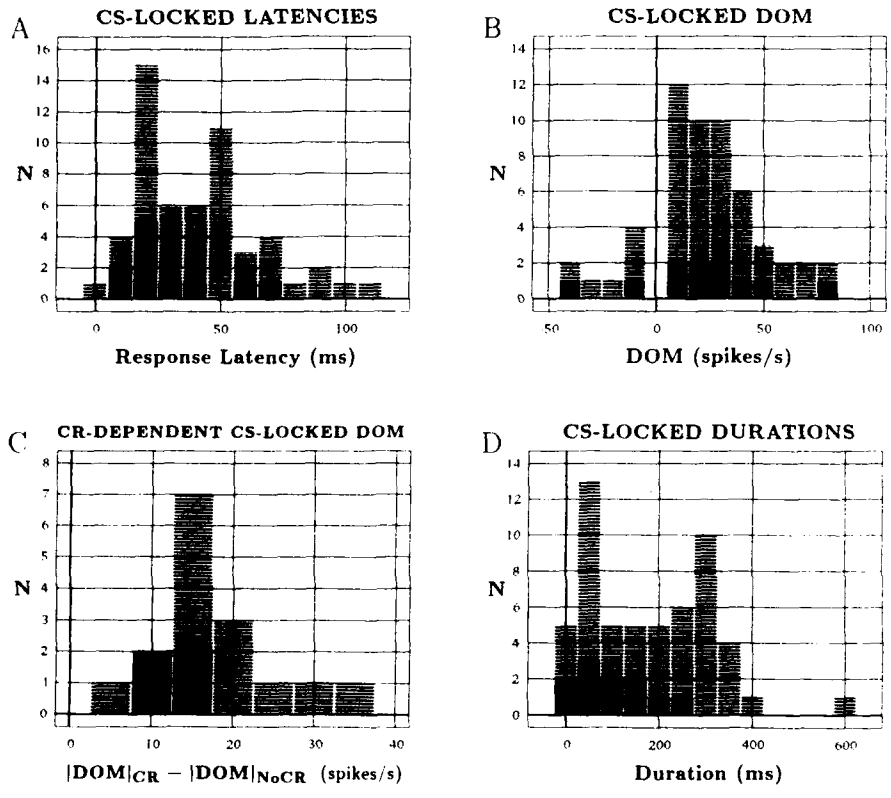

Fig. 4. Frequency histograms for CS-locked changes in firing. For all graphs, solid bars represent select subpopulation units. (A) Frequency distribution of response latencies for CS-locked changes in firing. The x-axis represents time in ms measured from CS onset. Both CR-dependent and non-CR-dependent responses are represented. (B) Depth of modulation (DOM) frequency distribution for all CS-locked changes in firing. Both CR-dependent and non-CR-dependent responses are represented. The x-axis depicts DOM in spikes/s; positive numbers represent an increase in firing relative to baseline and negative numbers represent a decrease. (C) Frequency distribution of increases in |DOM| on CR trials relative to non-CR trials for all CR-dependent CS-locked changes in firing. (D) Frequency distribution of durations of CS-locked changes in firing.

←Fig. 3. Raster plots of CS-locked changes in firing. Each row represents a different unit. Calibration marker represents 100 ms (x-axis) and 100 spikes/s (y-axis) for all graphs. (A) and (B) CS+ peri-stimulus plot and CS− peri-stimulus plot, respectively, for a unit that exhibited a CR-dependent CS-locked change in firing. For these and subsequent peri-stimulus graphs, the frequency of the CS (1200 or 600 Hz) and whether or not it was paired with the US (+ or −) appears at the top of the graph. The onset of the CS and US are indicated by vertical lines (for CS− the second vertical line represents CS offset). The onset of CS-locked firing is indicated by the arrow in (B). The firing is CR-dependent because the CS-locked firing is faster on CR trials than on no-CR trials (compare CR spikes with no-CR spikes). (C) and (D). CS+ and CS− peri-stimulus plots, respectively, for a unit that exhibited a non-CR-dependent CS-locked change in firing. (E) and (F) CS− peri-stimulus plot and peri-response plot, respectively, for a cell that exhibited a CR-dependent CS-locked change in firing followed by a CR-locked change in firing. The two changes are labelled in (E). For the graph in (F) and all subsequent peri-response plots, NM responses and spikes are depicted for CR trials only; NM responses and spike activity are shifted so that CR onset times are aligned. Note in (F) that increase in firing appears to the right of the CR onset line and, thus, the CR-locked firing lags the NM movement.

CS-locked changes in firing

A total of 55 units (44.0%) exhibited a change in firing that was time-locked to the CS onset. In 33 of these units, this was the only change in firing that occurred in the CS period. For example, the unit depicted in Figure 3A and B, and the unit in Figure 3C and D exhibited a CS-locked change in firing, but did not show a subsequent CR-locked change in firing. In 22 units, the CS-locked change preceded a second CR-locked change. An example of a unit a that exhibited CS-locked followed by CR-locked firing is depicted in Figure 3E and F.

Figure 4A illustrates the latency distribution of the CS-locked changes. The mean latency of the total distribution of units was 42.1 ms (median = 38.0 ms, SD = 25.4 ms). The latencies for the select subpopulation were not significantly different from those of the rest of the units (Mann-Whitney $U(11, 44) = 150$, $P > 0.05$, two-tailed).

For 39 of the 55 units that had a CS-locked change in firing, the rate of firing was the same regardless of whether or not a CR occurred. These units are referred to as *non-CR-dependent* CS-locked units. However, in 16 units, the DOM was greater when a CR occurred than when no CR was present, and these units are referred to as *CR-dependent* CS-locked units. The CS-locked firing for the unit depicted in panels A and B of Figure 3 was CR-dependent. This can be seen by comparing the CR spikes and the no-CR spikes during the CS period. As measured by cusums, the average firing rate on CR trials was 35 spikes/s greater than the rate on no-CR trials for this unit. The unit depicted in panel E also exhibited CR-dependent CS-locked firing. The CS-locked firing rate on CR trials was 15 spikes/s greater than the rate on no-CR trials. The CS-locked firing for the unit depicted in Figure 3C and D is non-CR-dependent. The median latency of CR-dependent CS-locked changes (53.0 ms) was slightly but significantly greater (Mann-Whitney $U(16, 39) = 188$, $P < 0.05$, two-tailed) than that of non-CR-dependent CS-locked changes (32.0 ms).

Figure 4B illustrates the distribution of DOM for the CS-locked changes. As in panel A of the figure, both non-CR-dependent and CR-dependent changes are combined. For the CR-dependent CS-locked changes, the DOM during CR trials are represented in the histogram. Negative numbers along the x-axis represent decreases in firing relative to baseline whereas positive numbers represent increases. The figure shows that for most units, CS-locked responses consisted of an increase in firing rate. The overall mean $|\text{DOM}|$ is 29.4 spikes/s (median = 26.0, SD = 18.5). The DOM distributions for CR-dependent and non-CR-dependent changes are not significantly different (Mann-Whitney $U(16, 39) = 240$, $P > 0.05$, two-tailed). There was also no significant difference between DOM for the select subpopulation and DOM for the rest of the units (Mann-Whitney $U(11, 44) = 234$, $P > 0.05$, two-tailed).

Panel C of Figure 4 illustrates, for all CR-dependent CS-locked changes, the distribution of increases in $|\text{DOM}|$ on CR trials compared to no-CR trials (*i.e.*, $|\text{DOM}|_{CR} - |\text{DOM}|_{noCR}$ appears on the *x*-axis). The mean of this distribution is 17.2 spikes/s (median = 15.0, SD = 7.5). That is, if a CR occurred on a trial, the CS-locked change in firing was, on average, 17.2 ms greater than it was if no CR occurred. Select subpopulation units did not differ significantly from non-select units (Mann-Whitney $U(4, 12) = 9$, $P > 0.05$, two-tailed).

Panel D of Figure 4 illustrates the distribution of durations for CS-locked changes. The mean of this distribution is 181.9 ms (median = 172.0, SD = 129.1). The median duration for select subpopulation units (111.0 ms) is significantly less than that of the remaining units (215.0 ms) (Mann-Whitney $U(11, 44) = 129$, $P < 0.05$, two-tailed test). In addition, CR-dependent changes, with a median duration of 259.5 ms, were significantly longer

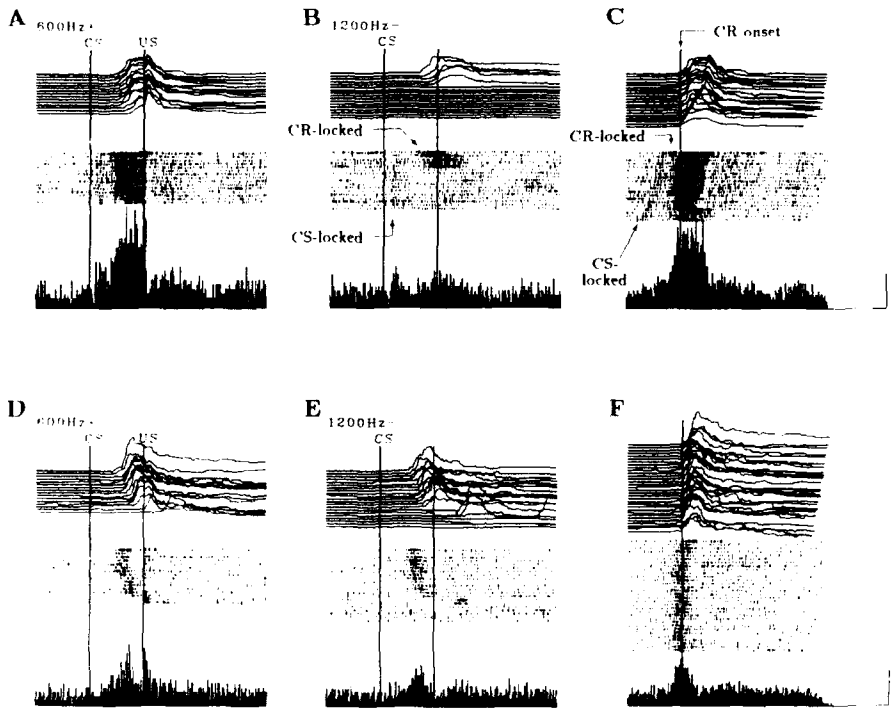

Fig. 5. Raster plots of CR-locked changes in firing. As in Fig. 3, each row represents a different unit. Calibration marker represents 100 ms (x-axis) and 100 spikes/s (y-axis) for all graphs. (A)–(C) CS+ peri-stimulus plot, CS− peri-stimulus plot, and peri-response plot, respectively, for a unit that exhibited a non-CR-dependent CS-locked change in firing followed by a CR-locked change in firing. In panels (B) and (C), CS-locked and CR-locked changes in firing are labelled. Note that in the peri-stimulus graph (B), onset of CS-locked firing occurs at relatively constant latency after CS onset and that onset of CR-locked firing is seen to shift as CR onset latency shifts. In the peri-response graph (C), CS-locked firing is shifted and CR-locked firing occurs at a relatively constant time prior to CR onset. (D)–(F) CS+ peri-stimulus plot, CS− peri-stimulus plot, and peri-response plot, respectively, for a unit that exhibited CR-locked, but not CS-locked, changes in firing.

than non-CR-dependent changes, which had a median duration of 125.0 ms (Mann-Whitney $U(16, 39) = 192$, $P < 0.05$, two-tailed test).

CR-locked changes in firing

A total of 59 units (47.2%) exhibited a change in firing that was time-locked to the CR onset. For 22 units, the CR-locked change was preceded by a CS-locked change. For 37 of these units, a single CR-locked change was the only change that occurred in the CS period. For example, panels A–C of Figure 5 illustrate a unit that exhibited a non-CR-dependent CS-locked change in firing that was followed by a CR-locked change. Panels D-F of the figure illustrate a unit that displayed only CR-locked firing.

Figure 6A illustrates the DOM distribution for all CR-locked changes. The figure reveals that most CR-locked responses consisted of an increase in firing rate. The mean |DOM| for the distribution is 38.1 spikes/s (median = 30.0, SD = 26.5).

Panel B of Figure 6 illustrates the distribution of lead times for all CR-locked changes. The x-axis represents the CR onset time (in ms) subtracted from the onset time of the change in firing, and, thus, negative numbers represent neural responses that lead the CR. The mean of this distribution is −35.8 ms (median = −33.0, SD = 49.7).

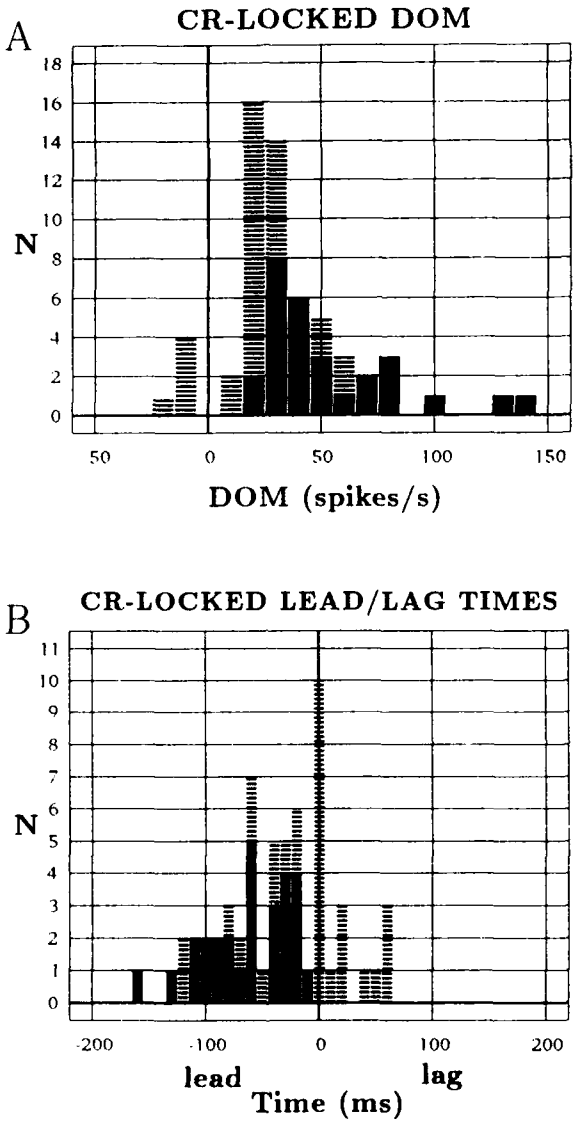

Fig. 6. Frequency histograms for CR-locked changes in firing. For all graphs, solid bars represent select subpopulation units. (A) Depth of modulation (DOM) frequency distribution for all CR-locked changes in firing. The x-axis represents DOM in spikes/s; positive numbers represent an increase in firing relative to baseline and negative numbers represent a decrease. (B) Frequency distribution of lead or lag times for all CR-locked changes in firing. The x-axis represents the time (ms) by which the onset of the CR-locked change preceded (negative numbers) or occurred after (positive numbers) the CR onset.

US-evoked responses

A total of 89 units (71.2%) responded to the US. The main types of responses that these units displayed were as follows: (a) 52 units (58%) exhibited an increase in firing to the US that lasted 20–200 ms and had DOM of 50–150 spikes/s. Panel A of Figure 7

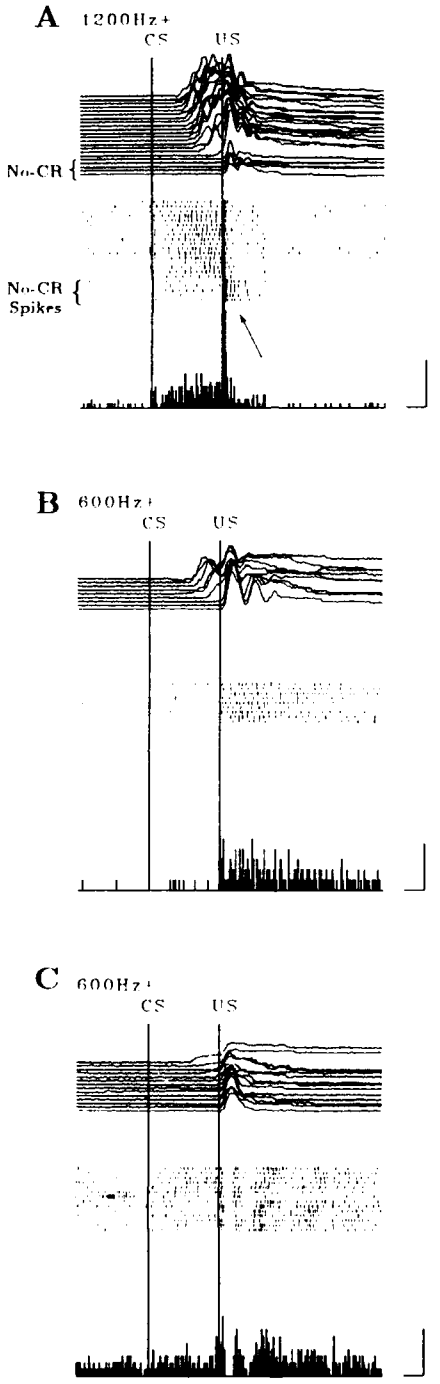

Fig. 7. US-evoked responses for 3 different units. Each graph is a CS+ peri-stimulus plot, and calibration marker represents 100 ms (x-axis) and 100 spikes/s (y-axis) for all graphs. (A) A unit that exhibited a CR-dependent US response. Note that the US response (indicated by arrow) was of greater duration on no-CR than on CR trials. (B) A unit that exhibited a long-lasting increase in firing to the US. (C) A unit that exhibited alternating increases and decreases in firing in response to the US.

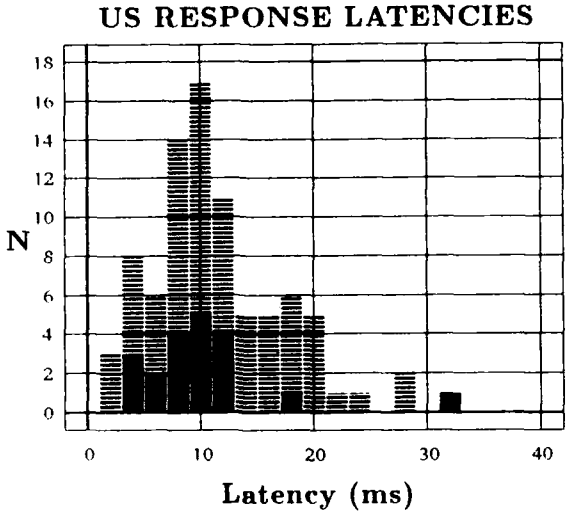

Fig. 8. Frequency distribution of response latencies for US-evoked changes in firing. The x-axis represents time in ms measured from US onset. Solid bars represent select subpopulation units. Four latencies ranging from 48–110 ms are not included in the figure.

illustrates an example of such a unit. (b) 23 units (26%) exhibited an increase in firing that lasted approximately 400 ms or more and had DOM of 40–60 spikes/s. An example of this type of US response is illustrated in panel B of Figure 7. (c) 14 units (16%) exhibited decreases in firing, or, more commonly, both increases and decreases in firing. Panel C of Figure 7 illustrates a unit that responds to the US with alternating increases and decreases in firing.

Figure 8 illustrates the distribution of onset latencies of US responses. Select and non-select subpopulations were not significantly different (Mann-Whitney $U(22, 67) = 650$, $P > 0.05$). The mean of the distribution is 14.3 ms (median = 10.2, SD = 14.7). The skewness of this distribution and the large standard deviation are attributable to 4 extreme values that ranged from 48–110 ms (these values do not appear in Fig. 8). If these data are not included, the mean US latency is 11.6 ms $\pm$ 6.0 ms SD. Because it takes about 9 ms for the eyeball to begin retraction after the US [51], the latencies of most of the US-evoked responses represented in Figure 8 were probably too short to be proprioceptive feedback from the UR. However, some of the late US responses may reflect feedback from the UR.

CR-dependent US responses

Because recordings were conducted before rabbits learned to completely differentiate CS + from CS −, rabbits failed to make CRs on some CS + trials. Ten units exhibited a more intense and/or longer US response on CS + trials when the rabbit failed to make a CR than when the animal did make a CR. The mean difference in firing rate during the first 50 ms of the US-evoked response on no-CR trials versus CR trials was 92.9 spikes/s (median = 69.1 SD = 60.3).

Panel A of Figure 7 illustrates a CR-dependent US response. Note in the graph that there are no CRs for the bottom 5 trials, and that the neuronal response to the US on these trials (indicated by arrow) is longer in duration than on CR trials. Another example of a CR-dependent US response can be seen in Figure 5D.

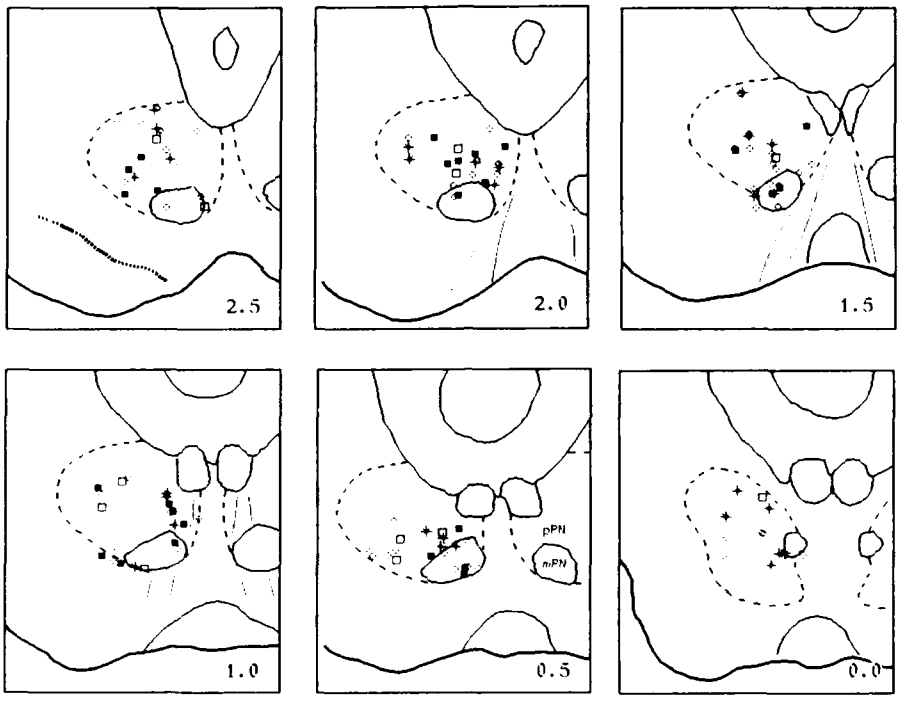

Fig. 9. Anatomical distribution of recording sites, with the units of the select subpopulation represented by asterisk symbols. Units that were not in the select subpopulation are depicted as follows. Open circles represent units with no apparent CR-related activity. Open squares represent units with CR-dependent CS-locked firing. Solid squares represent units with CR-locked firing, including units that had an initial non-CR-dependent CS-locked response followed by a CR-locked response. The figure depicts coronal sections through the brainstem with numbers in the bottom right corner of each panel indicating the distance in mm rostral to the posterior pole of the red nucleus. Magnocellular (mRN) and parvocellular (pRN) regions of red nucleus are denoted according to Gerhard[21].

Recording sites

Figure 9, which depicts coronal sections through the midbrain, illustrates the recording sites for the units reported in this study. Recordings were made from the caudal two-thirds of the red nucleus. The numbers in the bottom right corner of each panel indicate the distance in mm rostral to the posterior pole of the red nucleus. Magnocellular and parvocellular borders, based upon Gerhard's [21] rabbit atlas, are included, and are labelled mRN and pRN, respectively, in the 0.50 mm section.

In Figure 9, asterisks (*) depict units of the select subpopulation. It can be seen in this figure that several of the select subpopulation units were recorded from dorsal aspects of the magnocellular division. These units were located in what has been described as a 'face area' in cat red nucleus [53]. However, other select subpopulation units were lateral or ventral to the face area. The units that were not in the select subpopulation are depicted in Figure 9 as follows: (a) units that did not exhibit any CR-related firing (i.e., neither CR-locked firing nor CR-dependent CS-locked firing) are depicted as open circles; (b) units that displayed CR-dependent CS-locked firing are depicted as open squares; (c) units that displayed a non-CR-dependent CS-locked change followed by a CR-locked

change, or a CR-locked change alone, are depicted as filled squares. There is considerable overlap in the anatomical distribution of the types of units.

DISCUSSION

The results of this experiment can be summarized as follows:

(1) 89% of the units (111 units) exhibited at least one change in firing in either the CS period, the US period, or in both periods. Both CS-locked and CR-locked changes in the CS period were observed.
(2) CS-locked changes typically occurred 20–50 ms after CS onset and consisted of an increase in firing of 10–30 spikes/s above baseline.
(3) About one-third of all CS-locked changes were CR-dependent. For these responses, the firing rate was typically 15 spikes/s faster on CR trials than on no-CR trials.
(4) CR-locked changes typically consisted of a 20–40 spikes/s increase in firing rate above baseline. The lead time of the neuronal burst relative to CR onset varied considerably across units, with typical values of 0–60 ms.
(5) Overall, 54% of the units (67 units) exhibited some form of CR-related change(s) in firing during the CS period. The breakdown of these 67 units is as follows: 55% (37 units) had a CR-locked change, 12% (8 units) had a CS-locked CR-dependent change, 12% (8 units) showed a CS-locked CR-dependent change followed by a CR-locked change, and 21% (14 units) showed a CS-locked non-CR-dependent change followed by a CR-locked change.
(6) Neuronal responses to the US typically consisted of short bursts (20–200 ms) of increased firing. However, some units exhibited longer-lasting increases in firing, and other units exhibited alternating increases and decreases in firing. Onset latencies of US-evoked responses were approximately 8–12 ms.
(7) Some of the US-evoked responses were CR-dependent. This dependency consisted of a greater response when the CR was absent than when it was present.

Our findings of CR-locked unit activity in the red nucleus are consistent with the hypothesis that the red nucleus participates with the cerebellum to influence or control CR expression. The fact that CR-related firing patterns have been reported for deep cerebellar nuclear cells [5,43], and that the deep nuclear cells are a major source of afferents to the red nucleus, suggests the possibility that the red nucleus may relay CR information originating from deep cerebellar nuclei or cerebellar cortex. However, given the feedback loop organization of cerebellar–brainstem circuitry, it is difficult to ascertain where conditioning originates, or to rule out the possibility that conditioning occurs simultaneously in several sites.

The presence of both CS-locked and CR-locked changes in firing in the red nucleus is similar to sensory and motor components of unit activity found in the motor cortex [17,35]. Houk [32] has proposed a cooperative control model of movement that accounts for the two response components. In this model, the red nucleus not only participates in a positive feedback loop with lateral reticular nucleus and deep cerebellar nuclei, but also receives sensory input that serves to trigger movement. Under this model, triggering input, which could be either a copy of motor cortical activity or could come directly from sensory sources, would evoke CS-locked firing. The triggering input initiates positive feedback within the loop that ultimately grows into a motor response. Participation in this positive feedback loop results in CR-locked changes in firing.

Houk's model can account for the different combinations of CS-locked and CR-locked unit activity observed in the red nucleus. Some red nucleus cells may not receive the triggering input, but may still be recruited through divergence in the feedback loop. Such cells would exhibit CR-locked firing, but not CS-locked firing. Alternatively, a red nucleus cell may receive the trigger and exhibit a CS-locked response, but may not participate in the feedback loop and, thus, would not exhibit a CR-locked response. CR-dependent CS-locked activity can be explained by noting that relatively strong CS-locked firing might easily recruit feedback loop activity and, hence, generate a CR. In contrast, if the CS-locked change is weak, successful recruitment may be relatively unlikely. The strength or weakness of the triggering input may be modifiable through synaptic plasticity.

Under this model, CRs would be generated by rubrobulbar projections to the contralateral brainstem. There are 3 possible routes by which these projections could elicit NM movement. The first is by projecting to the accessory abducens nucleus (AAN), which contains the motoneurons principally involved in the NM response [2,3,13]. In cats, stimulation of the red nucleus produces EPSPs in contralateral AAN neurons at monosynaptic latencies [26]. Holstege and Tan [30] report that with autoradiographical tracing methods in cats, projections are observed from the dorsomedial portion of the caudal red nucleus to the AAN. Projections close to AAN, but not to AAN itself, have been observed in HRP experiments using cats [53] and rabbits (Rosenfield and Moore, personal communication). However, due to the large dendritic fields of AAN neurons [27,38], these nearby projections could directly affect AAN neurons.

A second route by which the red nucleus could generate CRs is by projections to the contralateral facial nucleus. In particular, the intermediate subnucleus of the facial nucleus innervates muscles surrounding the eye and controls eyeblink [30,31]. Eyeblink and NM movement are highly correlated [41], which is perhaps attributable to the overlapping dendritic fields of AAN and the facial nucleus neurons [27]. Red nucleus projections to the facial nucleus have been observed in rabbits [44,45] as well as in cats [8,15,30,31,53] and other species. Dorsal portions of the red nucleus appear to terminate heavily in the intermediate facial subnucleus [30,31,53]. Consistent with these anatomical data, intermediate facial nucleus neurons respond with EPSPs at monosynaptic latencies to red nucleus stimulation [18]. Our recording sites are consistent with a red nucleus–facial nucleus route for generating CRs. As observed in Figure 9, many CR-related units were found in dorsal apsects of the red nucleus.

A third way that the red nucleus could generate NM/eyeblink output is by projections to trigeminal subnucleus oralis (SpoV). These projections have been described for cats [15] and observed in rabbits (Rosenfield and Moore, unpublished data). Richards, Ricciardi, and Moore [52] found CR-related increases in firing in 5 of 20 units that were recorded in SpoV, two of which preceded the CR onset. A larger proportion of CR-related firing (12 of 26 units) was observed in the adjacent parvocellular reticular formation. Interestingly, Davis and Dostrovsky [9] reported that stimulation of the contralateral red nucleus in cats inhibited somatosensory responses in 64 out of 73 SpoV neurons and excited only 6 cells. Thus, although the data of Richards et al. [52] suggest that some SpoV cells may participate in CR generation, the Davis and Dostrovsky [9] results imply that the red nucleus–SpoV projection may also function to reduce responsiveness of SpoV to the US when CR-related red nucleus firing occurs. Such an effect might explain the CR-dependent US responses observed in some red nucleus units (see Fig. 7A).

As an alternative explanation for CR-dependent US responses, SpoV cells could project to red nucleus intrinsic inhibitory interneurons. If these interneurons fired in

response to movement-generated peripheral sensations, they would (a) decrease the firing of rubrobulbar neurons and thereby terminate the motor response, and (b) decrease the sensitivity of rubrobulbar neurons to an excitatory US input. SpoV-mediated inhibition of rubrobulbar neurons could account for the shortening of the CR duration that is observed when the US occurs [5]. Thus, some of the CR-lagging activity observed in the present study (see Fig. 6B) may be derived from inhibitory interneurons. A similar conclusion was reached by Otero and Lamas [49], who recorded red nucleus activity during forelimb extension movements in cats. They recorded movement-related increases in red nucleus firing in 40 of 81 cells; most of these cells increased firing after EMG onset of muscle responses. The red nucleus neurons were also tested for response to dentate/interpositus stimulation, and it was observed that the only red nucleus cells that responded to stimulation were the cells that did *not* exhibit movement-related activity. Because the only red nucleus cells that do not receive dentate/interpositus input are the inhibitory neurons, these neurons were thought to be the likely sources of the movement-related firing.

About two-thirds of our red nucleus units responded to the US. It is interesting to note that the shortest US response latencies in the red nucleus were less than the 5.5-ms minimum US response latency observed in the cerebellar nuclei [5]. In addition, the mean US response latency for cerebellar nuclear units is 14.5 ms $\pm$ 8.1 ms SD (range 9–34 ms) [5]. This value is nearly identical to the 14.3-ms mean latency observed for red nucleus units. * If red nucleus US responses were derived exclusively from deep nuclear cells, one would expect the mean red nucleus latency to be greater than that of the deep nuclear cells. A similar observation was made by Eccles et al. [14], who reported that the red nucleus latency distribution to stimulation of forelimb nerves was not shifted relative to nucleus interpositus latencies. Thus, our US latency results are consistent with the hypothesis that there are extracerebellar sensory projections to the red nucleus [50].

The CR-dependent US responses are of some theoretical interest, because these responses can be viewed as error-signals, reflecting the discrepancy between a teaching input (the US) and the current output of the system (the CR). Such error signals are at the core of many computational models of learning [59]. Our observations of large US responses when the CR was absent can be interpreted as a large discrepancy between the US signal and the system's output. In contrast, when a CR was present, the US response was smaller, reflecting a small error signal.

The CS-locked CR-dependent responses observed in this study are similar to those reported elsewhere. For example, Amalric et al. [1] and Schmied et al. [57] recorded red nucleus unit activity from cats that were trained to perform a forelimb flexion. An auditory CS was used to elicit the flexion response, and the response was rewarded if it occurred within 600 ms after the CS. These investigators observed CS-locked increases in firing rate at latencies of 40.8 ms $\pm$ 12 ms SD, which closely corresponds to the latencies observed in the present study (mean = 42.1 ms, median = 38.0 ms, SD = 25.4 ms). These CS-locked responses did not occur when the cat failed to make a flexion response. Most of their units also displayed a secondary response-locked increase in firing. In contrast to the results of Amalric et al. [1], about half of our CR-related units exhibited CR-locked responses but no CS-locked changes.

* In fact, if the 4 outlier US-response latencies for red nucleus units are excluded (see Results), the mean US response latency is 11.6 $\pm$ 6.0 ms, which is significantly *less* than the latency for deep nuclear units ($t(160) = -2.55$, $P < 0.05$, two-tailed test).

In summary, our results support the notion that the red nucleus is involved in the conditioned NM response, and the firing changes observed are consistent with Houk's [32] cooperative control model. However, questions remain as to how fine control could be exerted on the red nucleus–cerebellar nuclei positive feedback loop. Such control would be required to achieve the well-defined timing properties of CRs [25]. For example, CR onset is inhibited during the early portion of the CS–US interval, but emerges prior to US onset and peaks in amplitude at the time of US occurrence. Changes in the CS–US interval produce corresponding changes in the time course of the CR. Because of these temporal properties, we have suggested that adaptive timing mechanisms must be involved in the development of CRs [12], and we have hypothesized that such a mechanism could regulate the timing of Purkinje cell inhibition of deep cerebellar nuclei [47]. Such regulation applied to the cerebellar–brainstem feedback loop would permit fine control of the time course of CRs.

ACKNOWLEDGEMENTS

This research was supported by National Science Foundation grant BNS 88-10624 and Air Force Office of Scientific Research grant 89-0391. The authors wish to thank Marcy Rosenfield for histological assistance, and Drs. Neil Berthier and Bill Richards for comments on the manuscript. Thanks also to Dr. Ellen Stockman Desmond, who wrote the raster plot software in partial fulfillment of an NIMH postdoctoral fellowship payback obligation.

REFERENCES

1 Amalric, M., Conde, H., Dormont, J.F., Farin, D. and Schmied, A., Cat red nucleus changes of activity during the motor initiation in a reaction time task, *Exp. Brain Res.*, 52 (1983) 210–218.
2 Baker, R., McCrea, R.A. and Spencer, R.F., Synaptic organization of the cat accessory abducens nucleus, *J. Neurophysiol.*, 43 (1980) 771–791.
3 Berthier, N.E. and Moore, J.W., The nictitating membrane response: an electrophysiological study of the abducens nerve and nucleus and the accessory abducens nucleus in rabbit, *Brain Res.*, 258 (1983) 201–210.
4 Berthier, N.E. and Moore, J.W., Cerebellar Purkinje cell activity related to the classically conditioned nictitating membrane response, *Exp. Brain Res.*, 63 (1986) 341–350.
5 Berthier, N.E. and Moore, J.W., Activity of cerebellar deep nuclear cells during classical conditioning of nictitating membrane extension in rabbits, *Exp. Brain Res.*, 83 (1990) 44–54.
6 Burton, J.E. and Onoda, N., Dependence of the activity of interpositus and red nucleus neurons on sensory input data generated by movement, *Brain Res.*, 152 (1978) 41–63.
7 Clark, G.A., McCormick, D.A., Lavond, D.G. and Thompson, R.F., Effects of lesions of cerebellar nuclei on conditioned behavioral and hippocampal responses, *Brain Res.*, 291 (1984) 125–136.
8 Courville, J., Rubrobulbar fibres to the facial nucleus and the lateral reticular nucleus (nucleus of the lateral funiculus). An experimental study in the cat with silver impregnated methods, *Brain Res.*, 1 (1966) 317–337.
9 Davis, K.D. and Dostrovsky, J.O., Modulatory influences of red nucleus stimulation on the somatosensory responses of cat trigeminal subnucleus oralis, *Exp. Neurol.*, 91 (1986) 80–101.
10 Desmond, J.E. and Moore, J.W., Dorsolateral pontine tegmentum and the classically conditioned nictitating membrane response: analysis of CR-related activity, *Exp. Brain Res.*, 65 (1986) 59–74.
11 Desmond, J.E. and Moore, J.W., Red nucleus single-unit activity during the classically conditioned rabbit nictitating membrane response, *Soc. Neurosci. Abstr.*, 13 (1987) 841.
12 Desmond, J.E. and Moore, J.W., Adaptive timing in neural networks: the conditioned response, *Biol. Cybern.*, 58 (1988) 405–415.
13 Desmond, J.E., Rosenfield, M.E. and Moore, J.W., An HRP study of the brainstem afferents to the accessory abducens region and dorsolateral pons in rabbit: implications for the conditioned nictitating membrane response, *Brain Res. Bull.*, 10 (1983) 747–763.
14 Eccles, J.C., Scheid, P. and Taborikova, H., Responses of red nucleus neurones to antidromic and synaptic activation, *J. Neurophysiol.*, 38 (1975) 947–964.

15 Edwards, S.B., The ascending and descending projections of the red nucleus in the cat: an experimental study using the autoradiographic tracing method, *Brain Res.*, 48 (1972) 45–63.
16 Ellaway, P.H., An application of the cumulative sum technique (cusums) to neurophysiology, *J. Physiol. (Lond.)*, 265 (1977) 1P.
17 Evarts, E.V. and Tanji, I., Reflex and intended responses in motor cortex pyramidal tract neurons of monkey, *J. Neurophysiol.*, 39 (1976) 1069–1080.
18 Fanardjian, V.V. and Manvelyan, L.R., Peculiarities of cerebellar excitation of facial nucleus motoneurons, *Neurosci. Lett.*, 49 (1984) 265–270.
19 Foy, M.R. and Thompson, R.F., Single unit analysis of Purkinje cell discharge in classically conditioned and untrained rabbits, *Soc. Neurosci. Abstr.*, 12 (1986) 518.
20 Fromm, C., Evarts, E.V., Kroller, J. and Shinoda, Y., Activity of motor cortex and red nucleus neurons during voluntary movement. In O. Pompeiano and C.A. Marsan (Eds.), *Brain Mechanisms and Perceptual Awareness*, Raven Press, New York, 1981, pp. 269–294.
21 Gerhard, L., *Atlas des Mittel- und Zwischenhirns des Kaninchens*, Springer-Verlag, New York, 1968.
22 Ghez, C. and Kubota, K., Activity of red nucleus neurons associated with a skilled forelimb movement in the cat, *Brain Res.*, 129 (1977) 383–388.
23 Gibson, A.R., Houk, J.C. and Kohlerman, N.J., Magnocellular red nucleus activity during different types of limb movement in the macaque monkey, *J. Physiol. (Lond.)*, 358 (1985) 551–570.
24 Gibson, A.R., Houk, J.C. and Kohlerman, N.J., Relation between red nucleus discharge and movement parameters in trained macaque monkeys, *J. Physiol. (Lond.)*, 358 (1985) 551–570.
25 Gormezano, I., Kehoe, E.J. and Marshall, B.S., Twenty years of classical conditioning with the rabbit, *Prog. Psychobiol. Physiol. Psychol.*, 10 (1983) 197–275.
26 Grant, K. and Horcholle-Bossavit, G., Red nucleus inputs to retractor bulbi motoneurones in the cat, *J. Physiol. (Lond.)*, 371 (1986) 317–327.
27 Gray, T., McMaster, S., Harvey, J. and Gormezano, I., Localization of retractor bulbi motoneurons in the rabbit, *Brain Res.*, 226 (1981) 93–106.
28 Haley, D.A., Thompson, R.F. and Madden, J., Pharmacological analysis of the magnocellular red nucleus during classical conditioning of the rabbit nictitating membrane response, *Brain Res.*, 454 (1988) 131–139.
29 Harkness, J.E. and Wagner, J.E., *The Biology and Medicine of Rabbits and Rodents*, 2nd edn., Lea and Fediger, Philadelphia, PA, 1983.
30 Holstege, G. and Tan, J., Projections from the red nucleus and surrounding areas to the brainstem and spinal cord in the cat. An HRP and autoradiographical tracing study, *Behav. Brain Res.*, 28 (1988) 33–57.
31 Holstege, G., Tan, J., Van Ham, J. and Bos, A., Mesencephalic projections to the facial nucleus in the cat. An autoradiographic tracing study, *Brain Res.*, 311 (1984) 7–22.
32 Houk, J.C., Cooperative control of limb movements by the motor cortex, brainstem and cerbellum. In R.M.J. Cotterill (Ed.), *Models of Brain Function*, Cambridge University Press, Cambridge, 1989, pp. 309–325.
33 Houk, J.C. and Gibson, A.R., Sensorimotor processing through the cerebellum. In *New Concepts in Cerebellar Neurobiology*, Alan R. Liss, Inc., New York, 1987, pp. 387–416.
34 Kohlerman, N.J., Gibson, A.R. and Houk, J.C., Velocity signals related to hand movements recorded from red nucleus neurons in monkey, *Science*, 217 (1982) 857–860.
35 Lamarre, Y., Busby, L. and Spidalieri, G., Fast ballistic arm movements triggered by visual, auditory and somesthetic stimuli in the monkey. I. Activity of precentral cortical neurons, *J. Neurophysiol.*, 50 (1983) 1343–1358.
36 Lavond, D.G., McCormick, D.A. and Thompson, R.F., A nonrecoverable learning deficit, *Physiol. Psychol.*, 12 (1984) 102–110.
37 Lavond, D.G. and Steinmetz, J.E., Acquisition of classical conditioning without cerebellar cortex, *Behav. Brain Res.*, 33 (1989) 113–164.
38 Lewis, J.L., LoTurco, J.J. and Solomon, P.R., Lesions of the middle cerebellar peduncle disrupt acquisition and retention of the rabbit's classically conditioned nictitating membrane response, *Behav. Neurosci.*, 101 (1987) 151–157.
39 Martin, J. H. and Ghez, C., Red nucleus and motor cortex: parallel motor systems for the initiation and control of skilled movement, *Behav. Brain Res.*, 28 (1988) 217–223.
40 Massion, J., Red nucleus: past and future, *Behav. Brain Res.*, 28 (1988) 1–8.
41 McCormick, D.A., Guyer, P.E. and Thompson, R.F., Superior cerebellar peduncle lesions selectively abolish the ipsilateral classically conditioned nictitating membrane/eyelid response of the rabbit, *Brain Res.*, 244 (1982) 347–350.
42 McCormick, D.A., Steinmetz, J.E. and Thompson, R.F., Lesions of the inferior olivary complex cause extinction of the classically conditioned eyeblink response, *Brain Res.*, 359 (1985) 120–130.

43 McCormick, D.A. and Thompson, R.F., Neuronal responses of the rabbit cerebellum during acquisition and performance of a classically conditioned nictitating membrane-eyelid response, *J. Neurosci.*, 4 (1984) 2811–2822.

44 Mizuno, N., Mochizuki, K., Akimoto, C., Matsushima, R. and Nakamura, Y., Rubrobulbar projections in the rabbit. A light and electron microscopic study, *J. Comp. Neurol.*, 147 (1973) 267–280.

45 Mizuno, N. and Nakamura, Y., Rubral fibers to the facial nucleus in the rabbit, *Brain Res.*, 28 (1971) 545–549.

46 Moore, J.W. and Desmond, J.E., Latency of the nictitating membrane response to periocular electrostimulation in unanesthetized rabbits, *Physiol. Behav.*, 28 (1982) 1041–1046.

47 Moore, J.W., Desmond, J.E. and Berthier, N.E., Adaptively timed conditioned responses and the cerebellum: a neural network approach, *Biol. Cybern.*, 62 (1989) 17–28.

48 Otero, J.B., Comparison between red nucleus and precentral neurons during learned movements in the monkey, *Brain Res.*, 101 (1976) 37–46.

49 Otero, J.B. and Lamas, A.C., Red nucleus unitary activity during ballistic movements. Effect of cerebellar nuclei stimulation, *Brain Res.*, 248 (1982) 387–391.

50 Padel, Y., Sybirska, E., Bourbonnais, D. and Vinay, L., Electrophysiological identification of a somaesthetic pathway to the red nucleus, *Behav. Brain Res.*, 28 (1988) 139–151.

51 Quinn, K.J., Kennedy, P., Weiss, C. and Disterhoft, J., Eyeball retraction latency in the conscious rabbit measured with a new photodiode technique, *J. Neurosci. Meth.*, 10 (1984) 29–39.

52 Richards, W.G., Ricciardi, T.N. and Moore, J.W., Activity of spinal trigeminal pars oralis and adjacent reticular formation neurons during the classically conditioned rabbit nictitating membrane response. *Behav. Brain Res.*, 1991, in press.

53 Robinson, F.R., Houk, J.C. and Gibson, A.R., Limb specific connections of the cat magnocellular red nucleus, *J. Comp. Neurol.*, 257 (1987) 553–577.

54 Rosenfield, M.E., Dovydaitis, A. and Moore, J.W., Brachium cunjunctivum and rubrobulbar tract: brain stem projections of red nucleus essential for the conditioned nictitating membrane response, *Physiol. Behav.*, 34 (1985) 751–759.

55 Rosenfield, M.E. and Moore, J.W., Red nucleus lesions disrupt the classically conditioned nictitating membrane response in rabbits, *Behav. Brain Res.*, 10 (1983) 393–398.

56 Rosenfield, M.E. and Moore, J.W., Red nucleus lesions impair acquisition of the classically conditioned nictitating membrane response but not eye-to-eye savings or unconditioned response amplitude. *Behav. Brain Res.*, 17 (1985) 77–81.

57 Schmied, A., Amalric, M., Dormont, J.F., Conde, H. and Farin, D., Participation of the red nucleus in motor initiation: unit recording and cooling in cats, *Behav. Brain Res.*, 28 (1988) 207–216.

58 Spencer, R.F., Baker, R. and McCrea, R.H., Localization and morphology of cat retractor bulbi motorneurons, *J. Neurophysiol.*, 43 (1980) 754–770.

59 Sutton, R.S. and Barto, A.G., Toward a modern theory of adaptive networks: expectation and prediction, *Psychol. Rev.*, 88 (1981) 135–170.

60 Tsukahara, N., Oda, Y. and Notsu, T., Classical conditioning mediated by the red nucleus in the cat, *J. Neurosci.*, 1 (1981) 72–79.

61 Turker, K.S. and Miles, T.S., Climbing fiber lesions disrupt conditioning of the nictitating membrane response in the rabbit, *Brain Res.*, 363 (1986) 376–378.

62 Yeo, C.H., Hardiman, M.J. and Glickstein, M., Classical conditioning of the nictitating membrane response of the rabbit. I. Lesions of the cerebellar nuclei, *Exp. Brain Res.*, 60 (1985) 87–98.

63 Yeo, C.H., Hardiman, M.J. and Glickstein, M., Classical conditioning of the nictitating membrane response of the rabbit. II. Lesions of the cerebellar cortex, *Exp. Brain Res.*, 60 (1985) 99–113.

64 Yeo, C.H., Hardiman, M.J. and Glickstein, M., Classical conditioning of the nictitating membrane response of the rabbit. IV. Lesions of the inferior olive, *Exp. Brain Res.*, 63 (1986) 81–92.